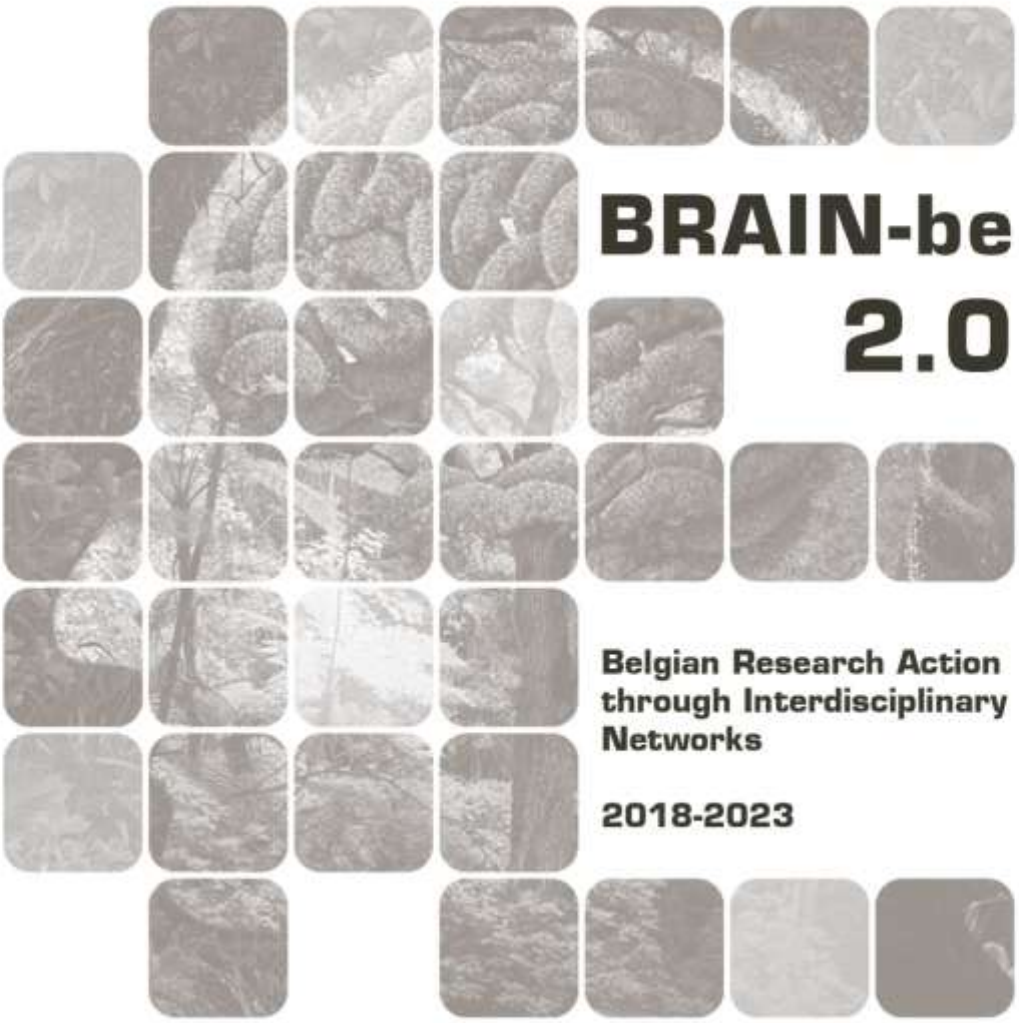

BG-PART

BioGeochemical PARTicle interactions and feedback loops on the Belgian Continental Shelf

Desmit, X. (RBINS), Sabbe, K. (UGent), De Rijcke, M. (VLIZ), Terseleer, N. (RBINS), Brun, A. (UGent), Dujardin, J. (VLIZ), Fettweis, M. (RBINS)

Pillar 1: Challenges and knowledge of the living and non-living world

belspo .be

NETWORK PROJECT

BG-PART

BioGeochemical PARTicle interactions and feedback loops on the Belgian Continental Shelf

Contract - B2/202/P1/BG-PART - B2/212/P1/BG-PART-2

FINAL REPORT

PROMOTORS: Xavier Desmit, Nathan Terseleer, Michael Fettweis (RBINS)
Koen Sabbe, Auria Brun, Wim Vyverman (PAE-UGent)
Maarten De Rijcke, Jens Dujardin (VLIZ)

AUTHORS: Desmit, X., Sabbe, K., De Rijcke, M., Terseleer, N., Brun, A., Dujardin, J., Fettweis, M.

Published in 2026 by the Belgian Science Policy Office
WTCIII
Simon Bolivarlaan 30 bus 7
Boulevard Simon Bolivar 30 bte 7
B-1000 Brussels
Belgium
Tel: +32 (0)2 238 34 11
http://www.belspo.be
http://www.belspo.be/brain-be

Contact person: Koen Lefever
Tel: +32 (0)2 238 35 51

Desmit, X., Sabbe, K., De Rijcke, M., Terseleer, N., Brun, A., Dujardin, J., Fettweis, M.,. ***BioGeochemical PARTicle interactions and feedback loops on the Belgian Continental Shelf***. Final Report. Brussels: Belgian Science Policy Office 2025 – 44

p. (BRAIN-be 2.0 - (Belgian Research Action through Interdisciplinary Networks))

Table of Content

1. Achieved Work

1.0. General introduction

BG-PART addressed the mutual interactions between plankton and suspended particulate matter (SPM) along the onshore-offshore gradient on the Belgian Continental Shelf (BCS). SPM is a mixture of mineral grains, microorganisms (such as bacteria and phytoplankton), detritus, adsorbed organic substances and xenobiotic particles (Ho et al., 2022; Silori et al., 2025a). While biology is affected by the variation in SPM concentration and composition, biological processes themselves can in turn impact SPM dynamics (Fettweis et al., 2022; Amadei Martinez et al., 2025). This may result in complex feedback loops affecting the functioning, services and habitability of the whole coastal ecosystem. In this project, we aimed to address major unresolved questions related to the interactions between biology and SPM dynamics in a shallow coastal ecosystem.

Main hypotheses:

Flocculation and transport of particles, including organic matter components and a variety of mineral particles, are strongly affected in the marine system by the SPM composition. The occurrence of organic matter, such as phytoplankton and derived detritus, correlates with enhanced flocculation in turbid systems (Amadei Martinez et al., 2025). During the growing season, phytoplankton and bacteria produce and excrete polysaccharides – or exopolymeric substances (EPS) – that can aggregate to form transparent exopolymer particles (TEP) which exhibit sticky properties and are known to foster larger floc formation (Engel et al., 2004; 2020). In turbid systems, however, it is assumed that the largest part of measured TEP is actually associated to clay particles, and more precisely these organic molecules are adsorbed on mineral surfaces. Such mineral-associated TEP is assumed to show no sticky properties, and only the freshly produced EPS and TEP will enhance flocculation (Fettweis et al., 2022). These hypotheses bear important consequences for the particle dynamics along the Belgian cross-shore gradient of SPM concentration, and hence for the capacity of phytoplankton to make photosynthesis in turbid waters. In turn, these interactions drive part of the carbon cycle on shelf seas (Regnier et al., 2013), and we attempt to clarify these issues. The following questions arise:

1. What phytoplankton species are found in the Belgian cross-shore gradient of turbidity, and how does the plankton community vary at seasonal and yearly time scales? **See section 1.1**
2. What are the optimal growth conditions of phytoplankton species, and under which conditions do phytoplankton communities produce marine gels and their precursors? **See section 1.2**
3. How do SPM, EPS and TEP concentrations vary in situ with the microbial community (phytoplankton and bacteria)? With what impact on flocculation, as determined by lab experiments? **See section 1.3**
4. What is the zooplankton community composition in the cross-shore gradient of SPM and across seasons? And what is their impact on the TEP concentration? **See section 1.4**
5. Coastal and offshore particles exhibit different composition in their organic and mineral contents. How do physical conditions influence organic and mineral particle interactions to shape the cross-shore gradient of SPM concentration? **See section 1.5**
6. By representing the plankton-particle interactions within a numerical 0D model representing a virtual water column, what can we say about the feedback interactions between plankton and particle dynamics? **See section 1.6**
7. Knowing that, in turbid systems, a substantial part of the organic carbon is associated by adsorption to mineral surfaces (clays) and therefore constitutes a carbon stock in the water column, how can we contribute to assess the carbon budget in the North Sea? **See section 1.7**

1.1. Phytoplankton community composition and dynamics in the BPNS from Jan 2022 – May 2023

1.1.1. Summary

Phytoplankton community composition depends on physical and chemical conditions of the environment and biotic interactions. Variability in these parameters drives seasonal cycles but can also induce short-term trends and interannual variability in species composition and size distribution of the phytoplankton community, which remains understudied. We examined variation in phytoplankton community composition across two consecutive spring blooms along a cross-shore gradient in the BPNS, using a multifaceted approach including eDNA metabarcoding, FlowCam, Imaging Flow Cytometry and pigment analysis. In both years, phytoplankton biomass and overall cell size decreased from coast to offshore. However, while the spring 2022 bloom cell numbers were dominated by chain-forming diatoms and the colony-forming haptophyte *Phaeocystis* spp., the bloom in spring 2023 was mainly dominated by mixotrophic (e.g., *Noctiluca*) and small-sized phytoplankton taxa (e.g., *Ostreococcus* spp. and *Micromonas* spp.), and an even stronger dominance of *Phaeocystis* spp. (especially offshore). In addition, in 2023 diversity was lower and the onset of the phytoplankton growing period was one month earlier than in 2022. We hypothesize that this interannual difference in spring bloom composition was linked to higher water temperature and overall lower nutrient concentrations in winter 2023 than in winter 2022. As a result, phytoplankton growth was sustained during winter 2023, leading to lower nutrient concentrations and limited spring growth. In conclusion, we saw a community shift towards smaller cells during the spring bloom linked to warmer winter conditions.

1.1.2. Environmental conditions and phytoplankton biomass

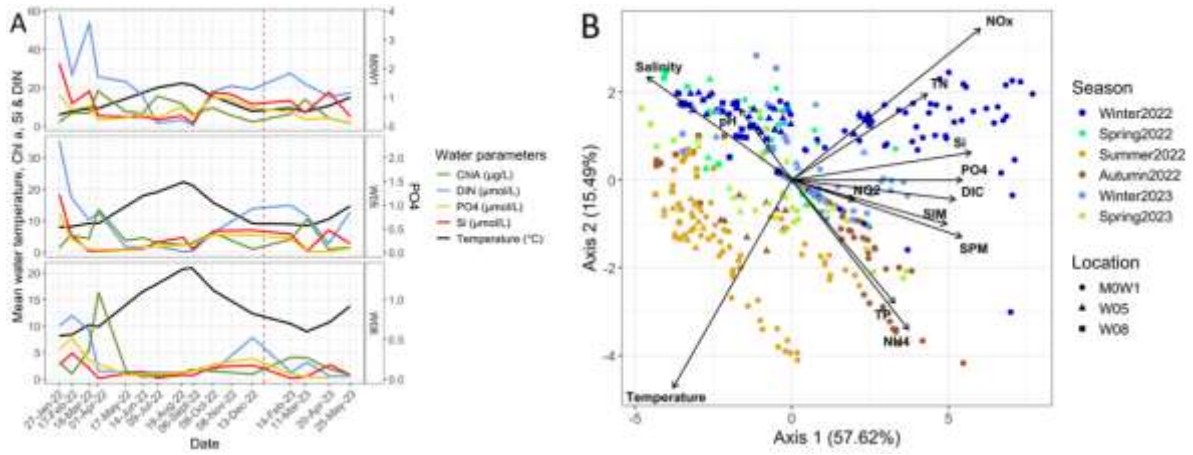

Figure 1 A: Water column parameters (chlorophyll a (Chl a – µg/L), dissolved inorganic nitrogen (DIN – µmol/L), mean water temperature (°C), phosphates concentration (PO_4 – µmol/L), silicates (Si – µmol/L)) measured at the three different sampling stations. Note the different scales for the three stations. B: Between-class analysis (BCA) biplot axes 1 and 2 based on abiotic environmental parameters (nitrogen oxides (NO_x – µmol/L), total nitrogen (TN – µmol/L), ammonium (NH_4^+ – µmol/L), nitrogen dioxide (NO_2 – µmol/L), phosphates (PO_4 – µmol/L), dissolved inorganic carbon (DIC – mg/L), silicates (Si – µmol/L), suspended particulate matter (SPM – mg/L) and suspended inorganic matter (SIM – mg/L), total phosphorus (TP – µmol/L), temperature (°C), salinity and pH).

We observed a cross-shore gradient, with higher DIN, DSi and PO_4 concentrations in the coastal zone than offshore (Fig.1). Mean water temperature in winter 2023 (ranging from 9 to 12°C throughout the

cross-shore gradient) was significantly higher than in winter 2022 (7 to 8°C). Nutrient concentrations showed an opposite pattern: mean values of dissolved DIN, DSi and PO_4 in winter 2023 were significantly lower than in winter 2022. Distinct spring blooms (Chl a peaks) occurred in March-April in the three stations, with additional less intense summer and autumn peaks in the coastal station, and a minor autumn peak in the transition station. No summer or autumn blooms were recorded in the offshore station. The spring bloom occurred about one month earlier in 2023 (March) than in 2022 (April), and was less intense, especially in the offshore station. However, while spring Chl a concentrations were significantly lower in spring 2023 than spring 2022 at W08, no significant difference was found between spring bloom Chl a concentration between 2023 and 2022 at MOW1 and W05.

In the between-class analysis (BCA), the cross-shore gradient is clearly visible, with the offshore station being characterized by higher salinity and pH, and the coastal station by higher SPM, Chl a and nutrient concentrations. There was a marked contrast between the winter and summer samples, with spring and autumn samples taking an intermediate position, depending on station and year. Interannual variability was pronounced: in spring 2022, the environmental conditions were still similar to those of winter 2022, while in spring 2023 conditions were more intermediate between winter and summer. Finally, we saw a wider range of variation in the coastal station MOW1 (clear distinction between the seasons) than in the offshore station W08.

1.1.3. Phytoplankton size distribution and abundance – Imaging Flow Cytometry data (I-FCM)

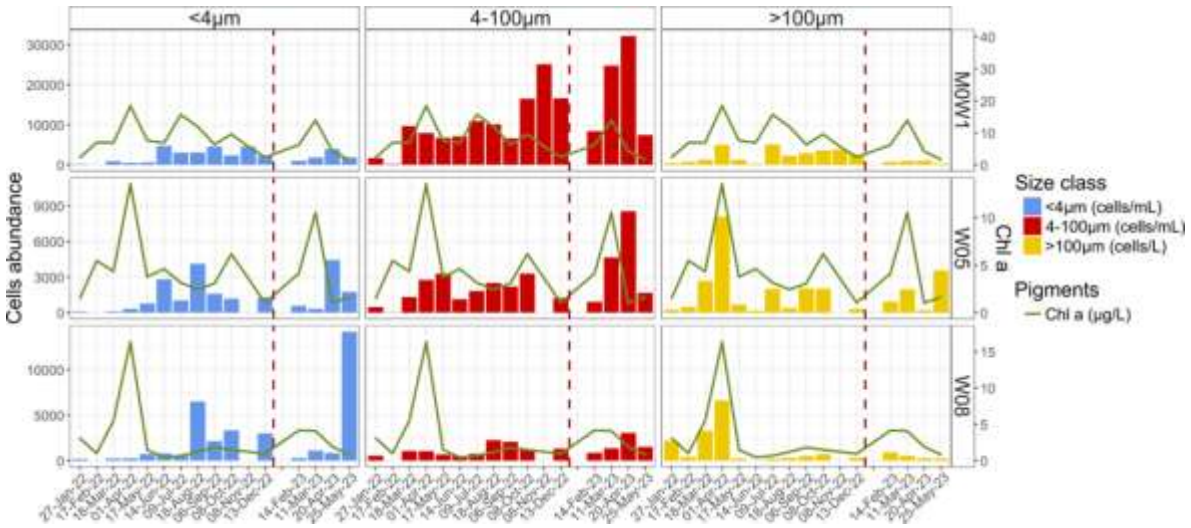

Figure 2 Pico- (<4 µm), nano/micro- (4-100 µm) and microphytoplankton (>100 µm) abundance (cells/mL) and Chl a concentration along the cross-shore gradient (MOW1, W05, and W08) during the period January 2022 to May 2023 (vertical dashed line separates 2022 and 2023). The picoplankton data are iFCM-based, nano/microplankton fractions is based on both iFCM and FlowCam, and the larger microplankton fraction is based on FlowCam data. NB: pico- and nano/microphytoplankton are expressed in cells/mL but microphytoplankton in cells/L.

Chl a concentration (~proxy phytoplankton biomass) was significantly correlated with the abundance of larger microplankton cells (>100 µm), but only marginally with that of cells between 4-100 µm (Fig.2). There was no significant correlation between Chl a and the abundance of picoplankton cells < 4 µm, nor between the different size classes. These data suggest that the bulk of the bloom biomass

is made up of larger microplankton cells and to a lesser extent nano/microplankton. There was a shift in cell size dominance (in terms of cell counts) both along the cross-shore gradient and between years. Coastal waters were dominated by large cells, with cell size decreasing as distance to the shore increased. Overall, cell size was larger in spring 2022 than 2023. Larger microphytoplankton (see below) abundance ranged from 1-18x10^3 cells/L, while pico- and smaller nano/microphytoplankton (iFCM) ranged from 0-32x10^3 cells/mL and 0-18x10^3 cells/mL respectively. The coastal station was characterized by nano/microphytoplankton in spring 2023, whereas in spring 2022 microphytoplankton was more important in terms of cell abundance. The transition station followed mostly the same pattern, but the picophytoplankton also represented a larger part of the spring 2023 community. Finally, the spring community of 2023 at the offshore station was vastly dominated by picophytoplankton, and to a lesser extent by nano/microphytoplankton, whereas the 2022 bloom was fully dominated by microphytoplankton.

1.1.4. Phytoplankton community structure and dynamics – eDNA metabarcoding and FlowCam (FC)

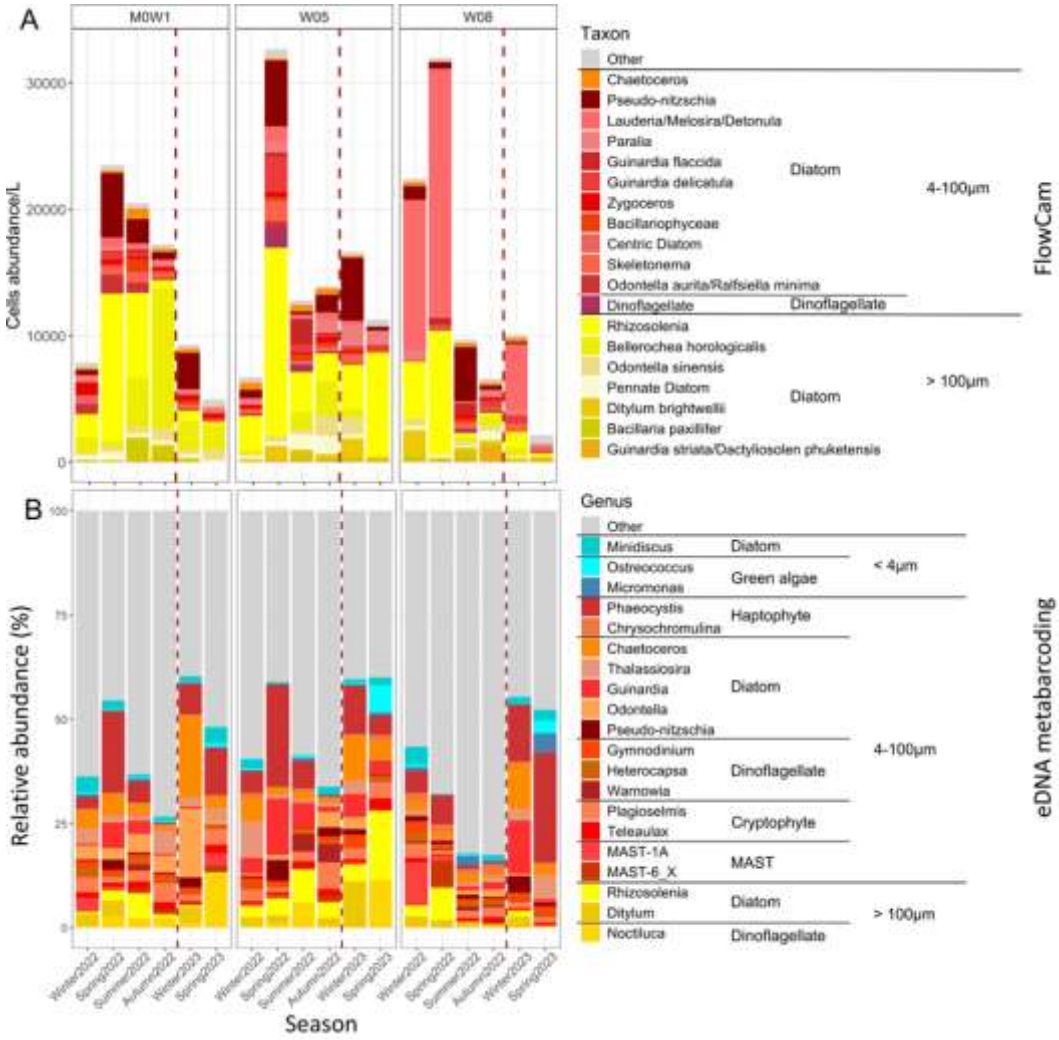

Figure 3 A: Abundance (cells/L) and community composition of microphytoplankton (FlowCam data, top 20 most abundant taxa, contributing to 90% of all detected cells) along the cross-shore gradient from January 2022 to May 2023. Size classes (i.e. in shades of red nano/microphytoplankton: 4-100 µm, and of yellow microphytoplankton: >100µm) are based on cell length (µm). B: Relative abundance of top 20 most abundant taxa (contributing about 60 % of read abundance in the entire dataset) in the eDNA

metabarcoding data set along the cross-shore gradient from January 2022 to May 2023. Size classes (shades blue: picophytoplankton <4 µm, shades of red: nano/microphytoplankton 4-100 µm, and shades of yellow: microphytoplankton >100µm) are based on cell length (µm).

Most genera were present all year round, but their relative abundance varied between stations and seasons (Fig.3). The winter 2022 community was characterized by the diatoms *Thalassiosira* spp., *Chaetoceros* spp., *Guinardia* spp., *Ditylum* spp., *Lauderia* spp. and *Minidiscus* spp. Microphytoplanktonic species (> 100 µm, shades of yellow in figure) were especially abundant in the spring 2022 bloom, but not in that of 2023. The haptophyte *Phaeocystis globosa* bloom in spring 2023 started one month earlier (March) than in spring 2022 (April)(data not shown). Summer 2022 was dominated by *Rhizosolenia* spp. (diatom). The autumn 2022 community was dominated in the coastal and transition zones by the diatom *Bellerochea horologicalis* and in the offshore zone by flagellates such as dinoflagellates (*Heterocapsa* spp.) or haptophytes (*Chrysochromulina* spp.). The community in winter 2023 was similar to that of winter 2022, however with a higher proportion of the diatoms *Ditylum* spp. and *Lauderia* spp. at W08, and *Guinardia* spp. at MOW1 and W05. *Chaetoceros* spp. were also found abundantly throughout the cross-shore gradient. The spring 2023 community was comprised of smaller cells such as the green algae *Ostreococcus* spp. and *Micromonas* spp. Furthermore, W08 was more dominated by *Phaeocystis* than the previous year, while MOW1 and W05 were dominated by the (heterotrophic) dinoflagellate *Noctiluca* sp.

1.2. Species-specific marine gel production in relation to light and temperature in phytoplankton from a well-mixed, turbid coastal system

1.2.1. Summary

We experimentally characterized the theoretical light-temperature niche of seven phytoplankton species (6 diatoms, 1 haptophyte) from the BPNS, and compared these to their realized niche in the BPNS, defined on the basis of metabarcoding data. We then investigated the production of dissolved sugars and marine gels (TEP and CSP) under optimal and suboptimal (upper and lower niche boundary) light and temperature conditions, and during exponential and stationary growth. We also determined the degree of bacterial colonisation of cells and gel aggregates. Interspecific differences in sugar and gel production were more pronounced than intraspecies variation related to variation in light, temperature and growth stage. Bacterial colonisation varied with marine gel composition. Maximum gel production often occurred under conditions that did not overlap with the realized light-temperature niches, which can affect *in situ* marine gel production. Marine gel production did not appear to be related to nutrient depletion, which contradicts the carbon overflow hypothesis. Instead marine gel production may be important to sustain the microbiome of the phytoplankton cells, which in turn provides the latter with molecules of interest, including remineralised nutrients. This could increase nutrient availability during post-bloom depletion.

1.2.2. Strain growth under different light and temperature conditions

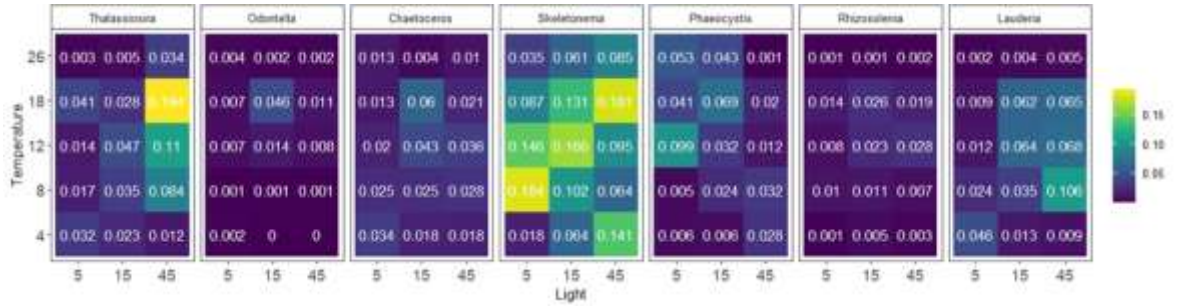

Figure 4 Maximum slope coefficient, i.e., growth rate in exponential phase (day^{-1}, colour legend), under different combinations of temperature (°C) (y-axis) and light (µmol.m^{-2}.s^{-1}) condition (x-axis).

The different species showed distinct light and temperature niches (differences in growth under a range of light and temperature conditions), and also pronounced differences in niche width (Fig.4).

1.2.3. Dissolved sugar and marine gel production, and bacterial colonisation in relation to temperature, light and growth stage

Significant differences were noted between the exponential and stationary phases in the raw and normalised (to Chl a and to particle area) total marine gel and precursor concentration data, with values consistently being either comparable or higher during the stationary phase compared to the exponential phase (Fig.5). However, this appears to be more related to accumulation than actual differences in the production rates. The lack of significant differences in precursor (sugar) and gel production rates between exponential and stationary phase (Jourdevant et al. 2025) does not support the carbon overflow theory as the main driver for polymer release, despite it being the most widely acknowledged theory (Engel, 2000; Underwood et al., 2004). Both inter- and intraspecies (i.e. between conditions and growth stage) differences were pronounced. However, differences in the production of marine gels and precursors per unit biomass were overall more significant between species than between conditions or between physiological states within a species.

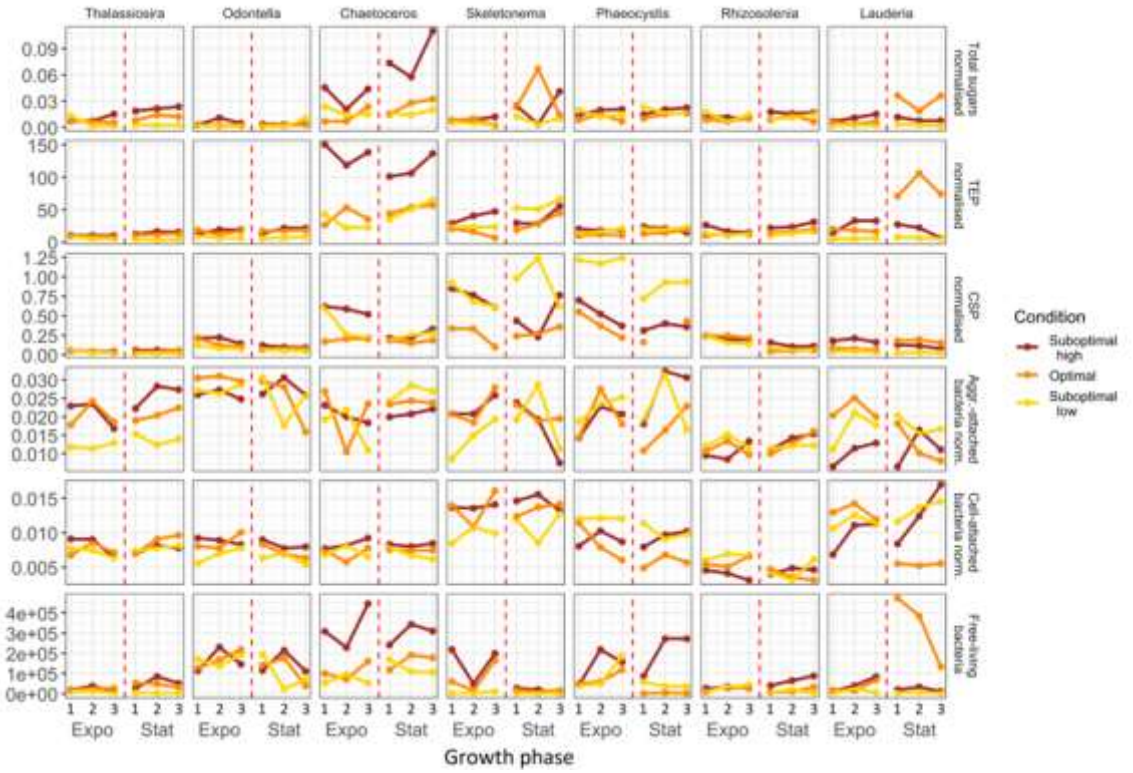

Figure 5 Normalised values of parameters measured during the exponential and stationary phase of the 7 selected strains: CSP:Chl a (mg BSA/µg chl a), TEP:Chl a (µg XG/µg ch la) & dissolved sugars:Chl a (mg glucose/µg chl a), as well as aggregate-attached bacteria:aggregate area (cells/µm²), cell-attached bacteria:cell area (cells/µm²) and free-living bacteria (cells/mL). The x-axis shows the three sampled days of each phase, under the label "Expo" for exponential phase and "Stat" for stationary phase.

Our results point toward a joint contribution in marine gel and precursor production from the different components of the phytoplankton community, with different species producing different substances in different conditions. Smaller phytoplankton cells have a higher capacity (normalized to biomass) for the production of marine gels and their precursors, and different species produce different marine gels. CSP production is entirely supported by these small cells. TEP production was ubiquitous, except in *Phaeocystis globosa*. The latter contrasts with other studies reporting high TEP production in this species (Chin et al., 2004; Mari et al., 2005). This discrepancy is most likely due to our strain not being colony-forming after months in culture.

1.2.4. Contribution of pico- and nanophytoplankton to TEP production

Over the course of 18 BG-PART campaigns, VLIZ performed 798 flowcytometry measurements, having the CytoSense flowcytometer setup to predominantly detect pico- and nanophytoplankton. By sheer cell numbers, the picophytoplankton dominated our data output (Fig.6). The offshore stations W05 and W08 tend to have more picophytoplankton than the nearshore station MOW1, where nanophytoplankton was relatively more common. In terms of biovolume, the nanophytoplankton had a much larger effect on total biomass than all other groups. Linear regression between the total biovolumes of each taxon and the TEP concentration of corresponding CTD-cast shows that TEP-concentrations correlate with both Pico-red (a polyphyletic group of small chlorophyll-containing cells) and Nano-SWS biovolume (mainly coccoliths). These preliminary conclusions need to be interpreted with care, however, as the analysis is flawed due to the selection bias against larger cells (e.g. diatoms belong to Micro-red) made by the instruments' settings. To fully comprehend the contribution of pico- and nanophytoplankton to TEP production on the Belgian Continental Shelf, we still need to add and

convert the phytoplankton observations made by the different groups of the consortium to get a full overview of all phytoplankton biomass.

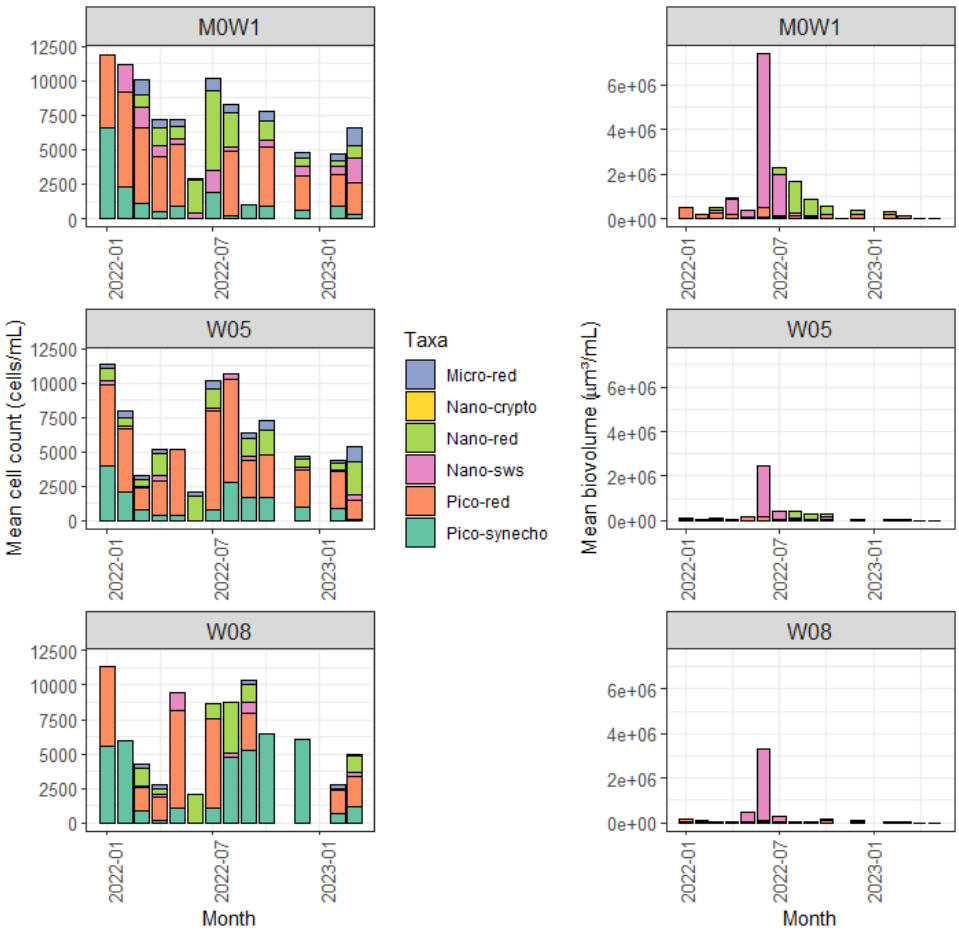

Figure 6 Evolution of the major functional groups of phytoplankton across all samples.

1.3. Spatial and temporal variation in SPM composition in relation to microbial (phytoplankton and bacterial) dynamics

1.3.1. Summary

We examined spatial and temporal variation in the SPM composition in the BPNS, using a 1 ½ year long monthly time series (Jan 2022 – May 2023) data set on floc abundance, composition and bacterial colonisation data along a cross-shore gradient. In addition, we performed a flocculation experiment using seawater obtained biweekly from the coastal station (MOW1) during the phytoplankton spring bloom of 2024. The flocculation potential of a water mass and its SPM were measured following the approach described in Amadei Martínez et al. (2025). We observed a gradient of organic content in the SPM, with lower content values in the coastal zone and higher values offshore, as the coastal zone

is highly turbid due to higher turbulence and the shallow, soft substrate sea bed. We also observed a seasonal pattern, with higher organic content in summer. Bacterial colonisation of flocs followed the same trend, as heterotrophic bacteria depend on OM availability. Our flocculation experiment showed a correlation between flocculation potential and the presence of phytoplankton and its exudates (i.e., marine gels), both higher in spring than winter. This supports that phytoplanktonic photosynthesis enhances flocculation at the seasonal scale, as suggested by Fettweis et al. (2022). However, the presence of marine gels was not correlated to larger flocs in the BPNS *in situ* time series. While this may be due to the low temporal resolution of sampling, it may also indicate that the stickiness of summer flocs, rich in marine gels, may impede tidally induced turbulence to resuspend large flocs which settled during low turbulence episodes.

1.3.2. Results

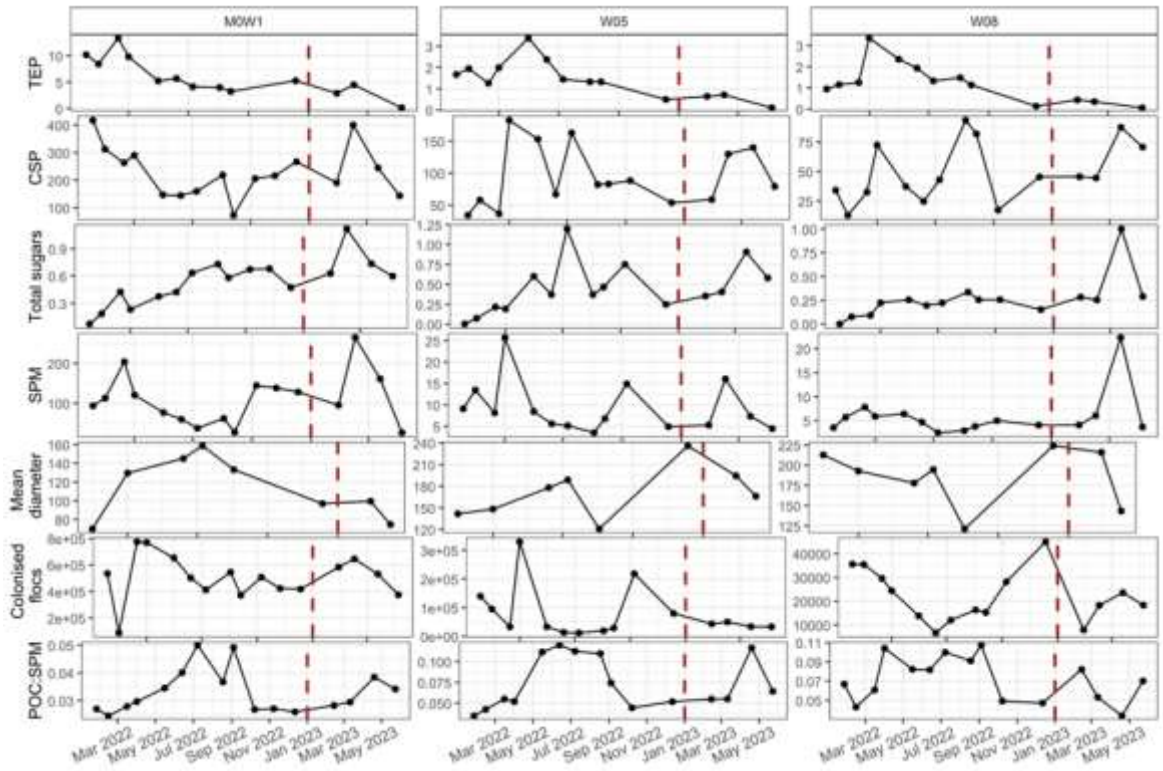

Figure 7 Raw data: TEP (mg XG/L), CSP (mg BSA/L), total dissolved sugars (mg/L) and SPM (mg/L) concentration, colonised flocs abundance (flocs/mL), mean SPM diameter (µm) and POC:SPM ratio (w/w); BNPS time series data set.

TEP concentration peaked in spring 2022, while no TEP peak was observed in spring 2023 (Fig.7). In 2022, total dissolved sugar concentration steadily increased to reach a maximal value in the summer. Interestingly, total dissolved sugar concentrations during spring 2023 showed a different pattern, with a sharp increase until March (at MOW1) or April (at W05 and W08), followed by a sharp decrease. CSP concentrations presented a strong gradient between MOW1 on the one hand and W05 and W08 on the other hand. At MOW1, CSP concentration was maximal in winter, while at W05 and W08, CSP peaked in spring and summer. SPM concentration was at its highest in winter to early spring at MOW1. SPM measurements at W05 and W08 showed a main peak in spring 2022, and a minor peak in summer 2022. Noticeably, values were three times higher at W08 in spring 2023 than spring 2022. The POC:SPM ratio was higher in summer than in the winter throughout the cross-shore gradient.

Total bacterial abundance (floc-attached and free-living, see examples of iFCM images in Fig.8) was positively correlated to Chl a concentration, with higher values in both parameters in the coastal station (Fig.9). Floc-attached bacteria numbers were up to 6x higher in the coastal station than in the offshore station. Free-living bacteria were up to 100x less abundant than floc-attached bacteria, and were up to 2x more abundant in the transition and offshore stations than in the coastal station. The coastal station was overall dominated by floc-attached bacteria and both free-living and floc-attached phytoplankton, while in the transition and offshore stations, the free-living heterotrophic fractions (bacteria and heterotrophs) were more important. Free-living bacterial abundance peaked in summer. Floc-attached bacteria peaked in spring to summer in the coastal station, and in winter and spring in the transition and offshore stations. Free-living phytoplankton and heterotrophs both peaked in spring. Bacterial densities on the colonised flocs (expressed per unit particle surface area, data not shown) also followed a seasonal pattern in the coastal station, with higher densities in summer than in winter, when POC:SPM values were also higher and SPM lower. This pattern, however, was not found at the transition and offshore stations. Interestingly, the overall highest values were reached in the transition station, followed by the offshore station and finally the lowest were in the coastal station.

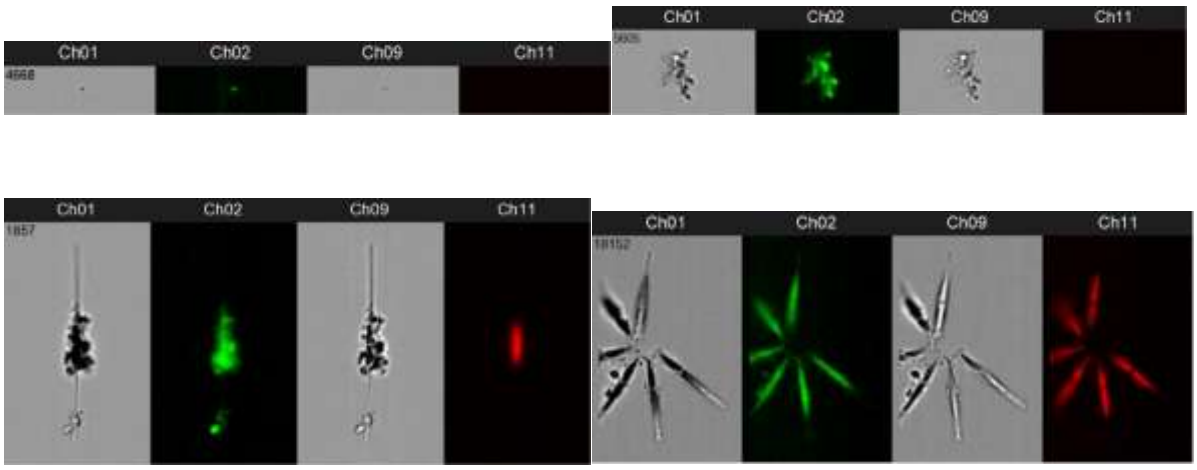

Figure 8: Example data acquired with imaging Flow Cytometry (iFCM). Channels indicate biological content of particles: Ch01 and Ch09 are Brightfield images at different focus depth, Ch02 is SybrGreen signal (DNA and RNA), Ch11 is autofluorescence signal (chloroplasts). Top row - particles without autotrophs <100µm: free living bacteria (left) & particles containing heterotrophs and/or mineral material colonised by bacteria (right). Bottom row - particles containing autotrophs <100µm: particles attached to and/or containing degraded phytoplankton (left) & free living, healthy phytoplankton (right).

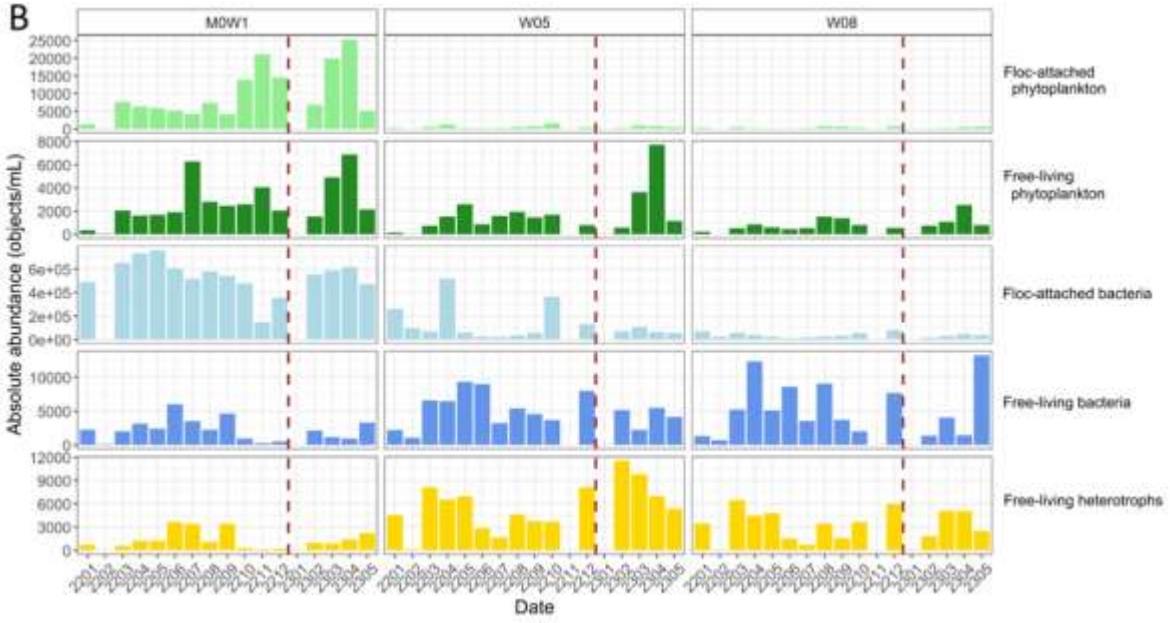

Figure 9 Absolute abundance (cells/mL) of the living organic component of the SPM (particle-associated and free living bacteria, floc-associated and free-living phytoplankton and free-living heterotrophs, all < 100 µm) present in the water column over the study period and the cross-shore gradient. The x-axis displays the sampling month, coded as "last two digits of the year, month number".

In the flocculation experiments (data not shown), total dissolved sugars and phytoplankton (cell abundance and Chl a concentration) increased from February to May 2024. Flocculation parameters [initial diameter, equilibrium diameter, flocculation efficiency (F_e), and flocculation velocity (V_f)] increased from February to late April, then decreased in May. CSP and TEP concentrations peaked twice: first in early March, then again in late April. V_f and F_e were both significantly positively correlated with phytoplankton abundance (free-living and floc-attached combined) and total dissolved sugar concentrations. F_e was significantly positively correlated with TEP and CSP concentrations.

1.4. Role of Zooplankton grazing

1.4.1. Summary

VLIZ participated in 18 sampling campaigns with RV Belgica, for a total of 37 days at sea, spread across the first two years of the project. In total, 193 net casts were performed for zooplankton analysis, capturing 31.507.191 scannable particles. Of those, 19,5 million particles were identified as detritus, 1.1 million were phytoplankton cells, and 641.552 were zooplankton organisms. The remaining items were either sediment, bubbles, fibres or other artefacts. Calanoid copepods are the dominant animal in plankton (51.7%; with density varying from 0.001 to 10 ind. l^{-1} and showing a maximum in July; with structurally higher abundance offshore), followed by small larvaceans as second common class (10.3%). No consistent tidal or diurnal pattern could be observed in copepod abundance at neither of the three stations. This may be attributed to the constant mixing of the water column possibly masking the copepod behaviour, and to patchiness in copepod distribution possibly blurring the sampling. Lab experiments show that the most common copepod in Belgian waters, *Acartia clausi*, can feed on TEP when starved in the absence of phytoplankton, but its impact remains low (<10% consumption of TEP in 48 h with an abundance of 10 ind. l^{-1}). We conclude that copepods do not have an important impact on TEP consumption at the tidal or seasonal scale.

1.4.2. Results

In line with expectations from the available literature on the North Sea and other marine ecosystems, the calanoid copepods were the dominant animal in the plankton, making up 51.7% of all counted individuals. Small larvaceans (Appendicularia) were the second most common class, contributing 10.3% of all individuals. Larval stages of echinoderms (8.5%) and barnacles (7.6%) were the third and fourth most common group, respectively. The last major group are harpacticoid copepods (6.4%). The remaining 15.6% is made up of various other organisms, including larvae from bivalves, crabs, worms, jellyfish etc. Calanoid densities varied between 0.001-10 per litre (Fig.10), with a clear peak in summer (July), which also matches the available literature for the Belgian Continental Shelf. Based on their size, behaviour and abundance, they are the most crucial grazer in the ecosystem.

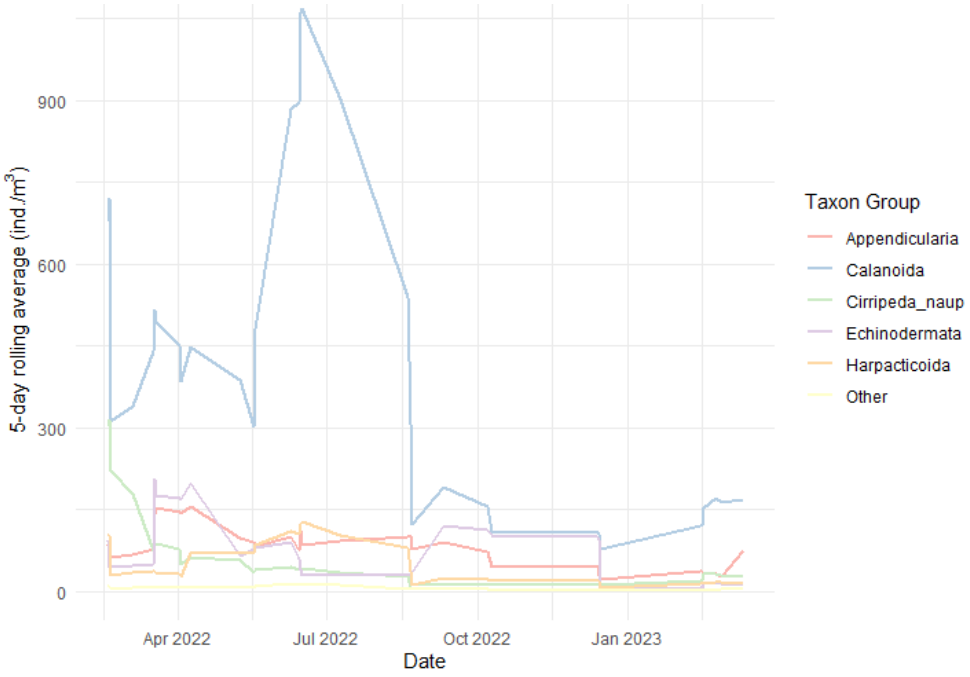

Figure 10 Smoothed seasonal trends of top 5 zooplankton groups across all samples.

For various reasons (e.g. weather, mishaps, operational restrictions), the sampling effort was unequally spread across stations and seasons. In total, 109 samples were taken at MOW1, 47 at W05, and 41 at W08. After losing a plankton net due to propellor entangling early in the BG-PART fieldwork, plankton sampling was only performed at the discretion of the captain of the ship, meaning data gaps exist across the tidal and seasonal scale. W08 had overall higher abundances of Calanoida than stations MOW1 and W05, which appears to be a structural trend (Fig.11). Going from offshore to nearshore, however, there is not a clear preference for deeper waters. Abundances at MOW1 exceeded those at W05 for roughly half of the time. Based on our data, it is not clear whether this is always the case, as MOW1 already started at elevated levels of abundances in early 2022, which may have a preceding ecological context which we did not capture.

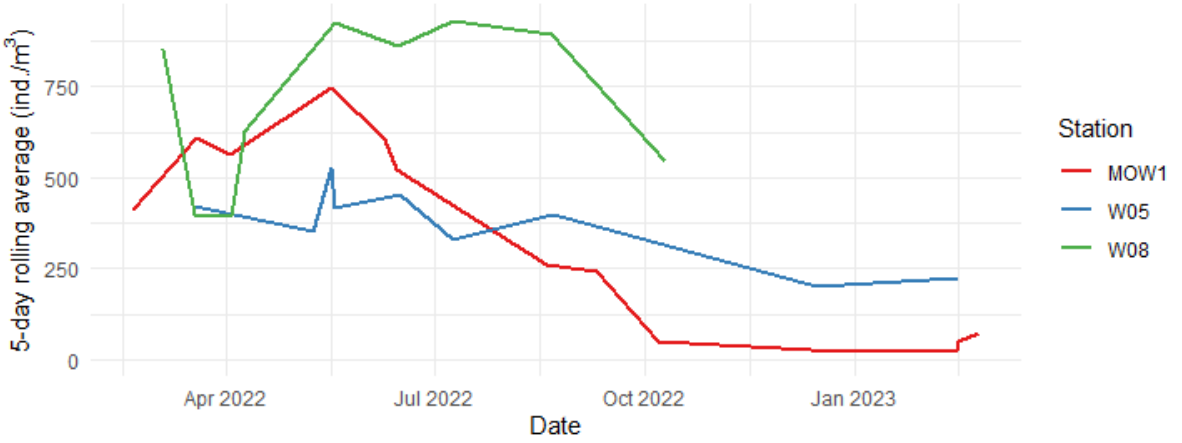

Figure 11 Smoothed seasonal trend of calanoid copepods in each of the three stations.

A key research question of the project, which could tie zooplankton grazing pressure to the observed fluctuations of TEP across tidal cycles, is whether copepod abundance shows a strong tidal signal. After the number of plankton casts was greatly reduced for operational reasons, we did not collect enough full tidal data series that can satisfactorily answer this question. MOW1, where we have the largest number of complete tidal cycle series, does not present a consistent picture (Fig.12). Assuming copepods should display tidal patterns, as described by some papers, the absence of such patterns at MOW1 can be caused by its shallow depth, allowing full vertical mixing of the water column which upsets the vertical pattern. At the deeper stations W05 and W08, which have limited data, we were also not able to distinguish a tidal signal (Fig.13). In rare cases, like the March campaign of 2022, we may have seen diurnal vertical movement, which is another known behaviour of copepods in the North Sea. This again is, however, not consistent throughout our data. It is not possible to distinguish tidal and diurnal behaviour from chance-based sampling of copepod clouds, which are known to be patchy and move with the water masses during tides. Based on all of this, we recommend that models for TEP use average abundances with a large (up to 300%) variation to sufficiently capture all variation.

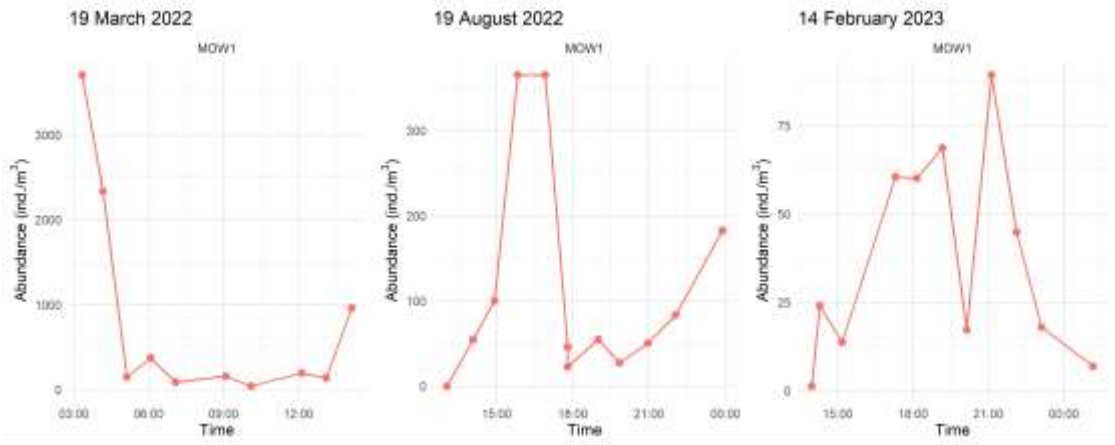

Figure 12 Examples of daily variation in calanoid copepod abundance at MOW1.

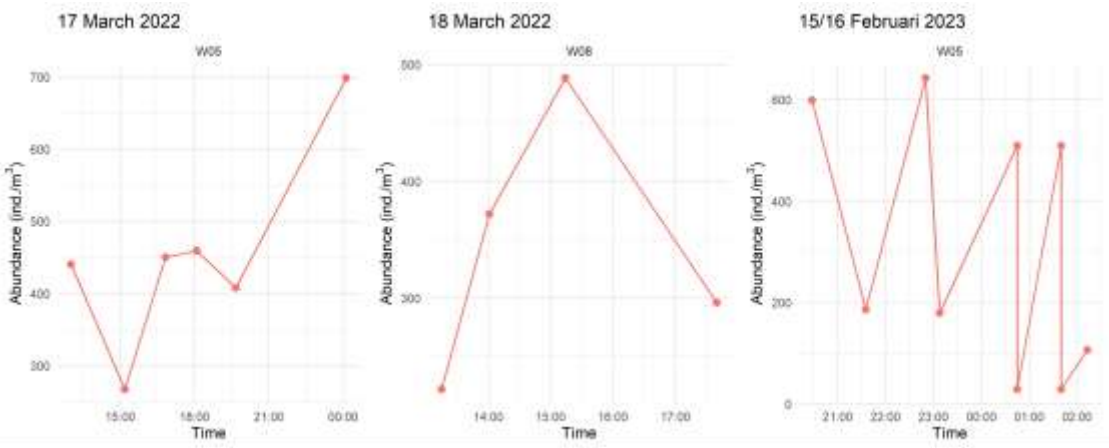

Figure 13 Examples of daily variation in calanoid copepod abundance at W05 & W08.

The scientific literature is conflicted about whether calanoid copepods consume TEP. During BG-PART, we conducted four grazing experiments in the lab with *Acartia clausi*, the most common copepod species found in the Belgian part of the North Sea. We found that *A. clausi* is capable of consuming TEP but will not feed on TEP when presented with an alternative food source (algae). Only after starvation will *A. clausi* feed on marine gels, releasing monosaccharides in the process. In a lab setting, the mechanical agitation caused by its swimming behaviour is capable of aggregating TEP from EPS precursors, a process which is likely irrelevant within turbid regimes like the North Sea. When TEP was consumed, the overall impact of 10 copepods per litre – a high abundance relative to the observations in the field – on TEP concentrations was less than 10% over 48 hours. Based on our lab experiments, it is not recommended to incorporate copepod grazing in models that predict TEP abundance in the North Sea.

1.5. The transition between coastal and offshore waters unraveled by suspended particle dynamics

1.5.1. Summary

Identifying the mechanisms that contribute to the variability of suspended particulate matter concentrations in coastal areas is important but difficult, especially due to the complexity of physical and biogeochemical interactions involved. This section addresses this complexity and investigates changes in the horizontal spread and composition of particles, focusing on cross-coastal gradients in the southern North Sea and the English Channel. A semi-empirical model is applied on in situ data of SPM and its organic fraction to resolve the relationship between organic and inorganic suspended particles. The derived equations are applied onto remote sensing products of SPM concentration, which provide monthly synoptic maps of particulate organic matter concentrations (here, particulate organic nitrogen) at the surface together with their labile and less reactive fractions. Comparing these fractions of particulate organic matter reveals their characteristic features along the coastal-offshore gradient, with an area of increased settling rate for particles generally observed between 5 and 30 km from the coast. We identify this area as the transition zone between coastal and offshore waters with respect to particle dynamics. Presumably, in that area, the turbulence range and particle composition favor particle settling, while hydrodynamic processes tend to transport particles of the seabed back towards the coast. Bathymetry plays an important role in controlling the range of turbulent dissipation energy values in the water column, and we observe that the transition zone in the southern North Sea is generally confined to water depths below 20 m. We refer to Desmit et al. (2024) for the whole study, including a description of the methods, the results, and the discussion.

1.5.2. Results

Using the model's best parameter estimates from a model of the particulate organic nitrogen (PON) content of SPM derived from Schartau et al. (2019) and Fettweis et al. (2022), we derived PON, PON_{ref} and PON_{fresh} concentrations from SPMC and applied it pixel wise to the satellite images in the southern North Sea and the English Channel. The uncertainties in the model parameters enhance the errors of the pixel wise values for PON_{fresh} and PON_{ref} in comparison with the satellite SPM concentration they are derived from. However, for geographical entities, which extend over tens of kilometres and comprise a larger number (10 to 100) of pixels, they still reveal robust patterns. We use ΔPON, the difference between PON_{ref} and PON_{fresh} concentrations (PON_{ref} - PON_{fresh}), to highlight the spatio-temporal variations of the PON dynamics and composition. It is shown for the months of January and April 2020 in Figure 14.

ΔPON varies in time and space as both fractions PON_{ref} and PON_{fresh} undergo biogeochemical transformations. In winter, ΔPON shows the highest values at the coast due to the dominance of PON_{ref} and rapidly decreases towards the offshore, where values are typically closer to zero as both PON_{ref} and PON_{fresh} are low and closer in concentration (Fig.14a). A notable exception offshore is the turbid Thames River plume carrying SPM from East Anglia across the sea to the German Bight and the coast of Denmark, and where PON_{ref} dominates. In the spring (Fig.14b), ΔPON shows its minimum values in a narrow area close to the coast. In that area, the freshly produced fraction of PON in spring is found in higher concentrations than PON_{ref}, which leads to negative values of ΔPON. While PON_{fresh} concentration in spring is a proxy for phytoplankton biomass, PON_{ref} always reflects the mineral fraction of SPM, which predominantly originates from resuspended sediment particles.

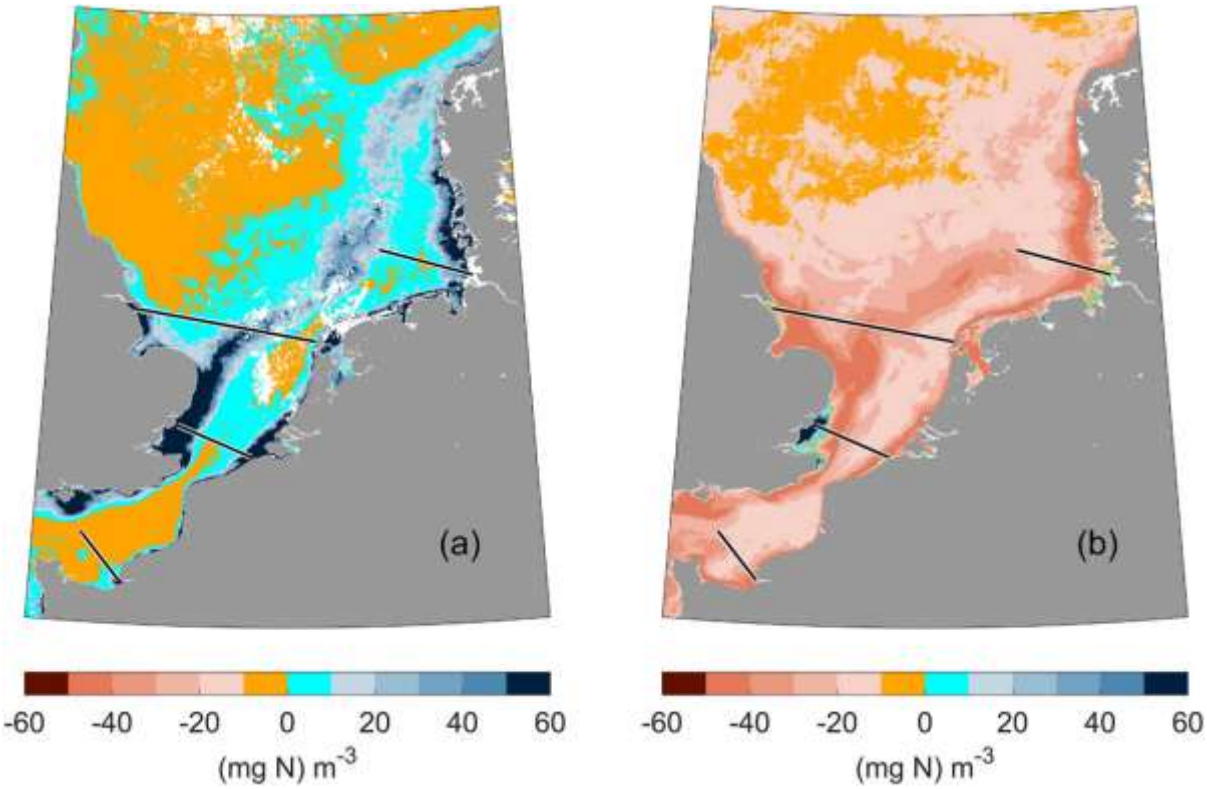

Figure 14 Surface ΔPON (PON_{ref}-PON_{fresh}) concentration [(mg N) m^{-3}] in 2020, January (a) and April (b).

Coastal areas with elevated SPM concentration, and with strong alongshore, weak cross-shore currents, and horizontal salinity gradients, feature a land-ocean transition zone that can be identified based on changes in particle compositions. Spatial and seasonal variabilities dominate the particle dynamics, suggesting that basin morphology and biological activity mainly control the processes at play. Bathymetry plays an important role in determining the turbulence effects on the flocculation and settling of particles. Our study shows that the coastal SPM concentration maximum and, thus, the maximum settling of particles generally occurs within depths below 20 m. The seasonal production of phytoplankton should enhance the particle settling and the accumulation of freshly produced particles at the bottom during the summer period. Due to vertical and horizontal density gradients and hydrodynamic (tidal) forcings, the particles in the transition zone may become subject to a near-bottom net transport towards the coast, hence maintaining the cross-shore gradient of particles. The offshore limit of the transition zone can thus be regarded as the 'line of no return' put forward by Postma (1984) across which any transport of SPM and its organic matter components becomes small throughout the year, especially in the growing season. The dynamics of particles in the transition zone influence the fate of organic matter. The freshly produced POM and a substantial part of the refractory POM tend to remain in the shallower areas of the coastal waters, while a minor fraction of the refractory POM is exported to the offshore during the winter. The impact of such particle dynamics on the carbon and nitrogen cycles in shelf seas should be further quantified in the future with additional data on vertical profiles modelling tools.

1.6. Numerical model of the plankton-sediment interactions

1.6.1. Summary

A new numerical model was built by coupling and adapting an existing biogeochemical model of plankton and an existing mineral model addressing particle flocculation. The modeled biological processes were parameterized based on literature data, while dedicated lab experiments were conducted in parallel to further investigate these processes (see section 1.2). The 0D box model was used both to interpret the lab experiments and to run scenarios, especially in conditions representing the turbid, well-mixed and eutrophied Belgian coastal zone. The model currently represents one phytoplankton functional group (diatoms), as this approach offers a good trade-off between reducing model complexity and achieving good results. The box model outcome shows a measurable impact of biologically-derived TEP on the particle dynamics in many aspects of the modeled processes, more specifically on the range and the time variability of the floc size. In turn, this induces changes in the SPM concentration and light penetration, which thus affects substantially phytoplankton photosynthesis, as shown by the applied scenarios. The model resolves both the tidal and seasonal time scales – an uncommon feature in particle modeling – and constitutes therefore a precious tool for further research on the topic.

1.6.2. Hypotheses and models

Our model addresses a fundamental challenge in coastal oceanography: understanding how biological processes influence SPM dynamics in highly turbid environments through complex feedback mechanisms involving TEP and marine gel production. Our primary objective is to develop a coupled biogeochemical-mineral flocculation model and investigate the relationships between SPM, TEP, and plankton across tidal and seasonal scales. Two complementary modeling applications are presented here:

1. Laboratory-scale TEP modeling: a biogeochemical model was used to simulate WP2 experiments with diatom cultures under varying conditions. This tested a project question by assessing how species with contrasting traits (e.g., light use, growth rates) can be represented within one framework, and whether the complexity of TEP production constrains its inclusion in models.
2. Ecosystem-scale coupled modeling: the full biogeochemical–flocculation model was applied in a box model representing the conditions of the coastal, turbid and eutrophied station MOW1 on the Belgian Continental Shelf. By incorporating organic (phytoplankton, bacteria, gels) and mineral components, the simulations evaluated one of the central BG-PART hypotheses that phytoplankton modify their physical environment to overcome growth limits, thus, reshaping ecosystem functioning in turbid coastal waters.

1.6.3. Constraining the model with lab experiments on phytoplankton

The biogeochemical model of Kerimoglu et al. (2022) was implemented in 0D to simulate WP2 laboratory experiments. The model includes nutrients (N, P, Si), diatoms, dissolved organic matter (DOM), TEP, detritus, and bacterial communities. Phytoplankton exudation produces DOM (equivalent to EPS) which aggregates to form TEP. TEP is lost through aggregation into detritus and bacterial consumption. Representing phytoplankton diversity poses challenges for model parameterization (Anderson, 2005). Given the limited representation of TEP dynamics in numerical models (Quigg et al., 2021), we tested whether a single model can simulate multiple species by applying two optimization approaches to the six diatom species across three light regimes from lab experiments: (1) individual optimization allowing species-specific parameters (maximum growth rate, photosynthetic efficiency,

mortality rate), and (2) common optimization using shared parameters across all species. Figure 15 shows results with individual optimization as continuous lines and common optimization as dashed lines. The model performs better with species-specific parameters than with common parameters. This is particularly evident for species with distinct growth dynamics: reduced growth (Chaetoceros in blue, Lauderia in orange, Skeletonema in purple) or delayed growth (Rhizosolenia, red). Despite these biomass simulation differences, the model outcome shows comparable TEP production in both cases. TEP is well simulated in both optimization approaches, with timing and magnitude matching observations. However, the model overestimates TEP levels for Skeletonema, possibly because of overestimated TEP production or missing TEP consumption pathways in the model. Biomass differences across light regimes do not translate into comparable TEP differences: TEP timing may vary, but magnitude remains consistent between light regimes in both simulations and observations (e.g., Lauderia). Model simulations show bacterial levels generally agreeing with observations but rapidly increasing toward experiment end, suggesting that bacterial emergence and effects on TEP dynamics require investigation over longer timescales.

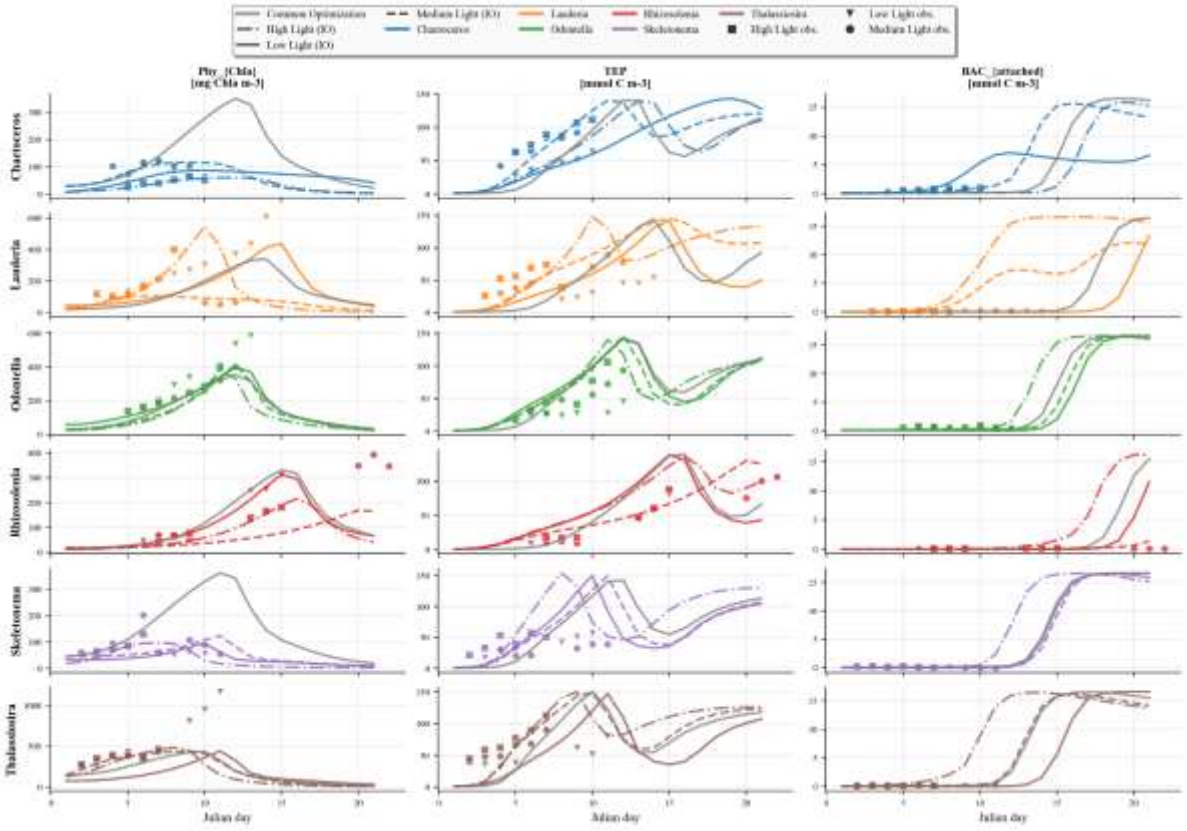

Figure 15 Model simulation of phytoplankton biomass (left), TEP (middle) and attached bacteria (right) for six diatom species (rows) under low, medium and high light regimes.

Figure 16 shows parameter values from both optimization approaches. Individual optimization yields growth rates spanning typical diatom values (<0.5 to >3 d^{-1}; e.g., Sarthou et al., 2005). Some patterns align with previous findings: Rhizosolenia shows the lowest growth rate (consistent with delayed biomass increase) and is associated with larger, slower-growing species, while Thalassiosira represents smaller, faster-growing early season species (Terseleer et al., 2014). Photosynthetic efficiency follows

similar patterns: smaller, early season species (Chaetoceros, Thalassiosira, Skeletonema) show higher efficiencies than larger, summer species like Rhizosolenia. Common optimization parameters cluster near median values, reflecting average behavior across species. Notably, optimized parameters for the same strain may vary between light regimes, indicating that physiological adaptations add complexity to biogeochemical model formulation and parameterization beyond interspecific diversity. However, TEP-related parameters were not calibrated and remained identical across all species and light regimes, yet produced reasonable results.

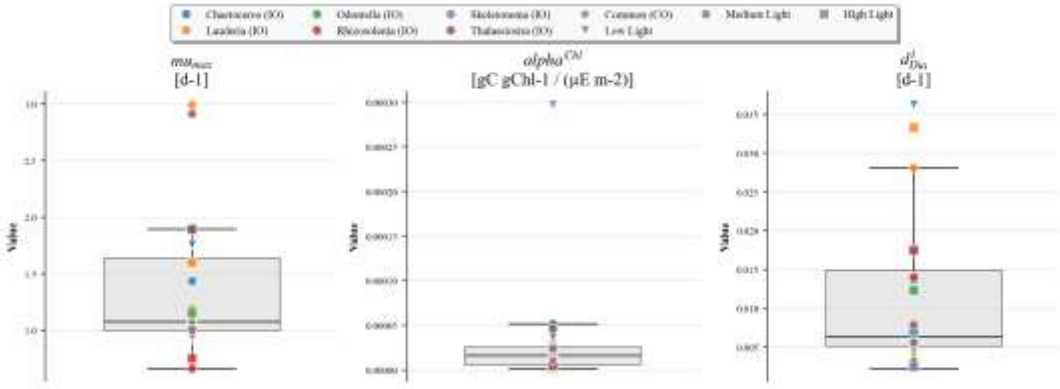

Figure 16 Optimized parameter values (growth rate, photosynthetic efficiency, mortality rate) for the individual (dots) and the common (squares) optimizations.

Altogether, while species-specific growth dynamics may be partially captured by globally-parameterized models, TEP production can be reasonably represented by a single parameterization. Therefore, the additional complexity needed to include TEP dynamics in biogeochemical models is limited while providing valuable insights for ecosystem-level studies. Accordingly, the model is applied to the Belgian coastal zone in the next section.

1.6.4. Ecosystem application at MOW1

The biogeochemical model of Kerimoglu et al. (2022) was implemented in 0D to simulate annual diatom and TEP dynamics at MOW1, a well-mixed shallow, turbid and eutrophied station (~12.5 m depth) in the Belgian coast. To account for high SPM levels and flocculation dynamics, the biogeochemical model was coupled to the Two-Class Population Balance Equation (TCPBE) mineral aggregation model of Lee et al. (2011). This model simulates the bimodal sediment size distribution through size-fixed microflocs and size-varying macroflocs. Macroflocs form through collision and aggregation processes and can break down into smaller components. Aggregation depends on both collision frequency and collision efficiency (fraction of collisions resulting in aggregation). This model has been successfully applied to Belgian coastal waters for tidal cycle SPM simulation (Lee, pers. comm.) and was coupled to a biogeochemical model for the first time in BG-PART. In the coupled biogeochemical-mineral flocculation model, TEP functions as biological "glue" modifying mineral flocculation through collision efficiency and floc strength enhancement. TEP-enhanced collision efficiency $\alpha(t)$ follows Michaelis-Menten kinetics:

$$\alpha(t) = \alpha^{ref} \times \frac{[TEP]}{K_{TEP}+[TEP]}$$

where $\alpha^{ref} = 0.05$ (reference collision efficiency), [TEP] is the simulated TEP concentration (mmol C m⁻³), and $K_{TEP} = 15\ mmol\ C\ m^{-3}$ (half-saturation constant). This saturation function prevents unrealistic infinite stickiness while allowing TEP-dependent collision enhancement with linear increase at low TEP concentrations.

Second, TEP strengthens flocs through time-varying yield strength $F_y(t)$:

$$F_y(t) = F_y^{base} + \Delta F_y^{max} \times \frac{[TEP]}{K_{TEP} + [TEP]}$$

where F_y^{base}= 1x10^{-10} N (base floc strength without TEP), and ΔF_y^{max}= 1x10^{-10} N (maximum TEP enhancement of floc strength). Thereby, TEP increases the force required to break particle bonds, adding polymeric bridging forces to the base forces between mineral particles (van der Waals and electrostatic forces).

With these effects on flocculation dynamics, TEP indirectly affects floc settling velocity by influencing floc size through enhanced aggregation. The settling velocity $w_s(t)$ follows the Winterwerp equation for fractal aggregates:

$$w_s(t) = \frac{1}{18} \times \frac{(\rho_s - \rho_w) \times g}{\mu_w} \times D_P^{3-n_f} \times D_F^{(n_f-1)}$$

where ρ_s= 2500 kg m⁻³ (microfloc particle density), ρ_w = 1025 kg m⁻³ (water density), g = 9.81 m s⁻² (gravitational acceleration), μ_w = 1002 mPa s (dynamic viscosity of water), D_P = 5x10^{-6} m (microflocs diameter), D_F is the floc diameter [m], and n_f = 2.1 (fractal dimension). The floc diameter D_F evolves as a function of the number of microflocs per macroflocs according to a fractal relationship.

Finally, considering that TEP creates a biofilm-like matrix at the sediment-water interface that increases cohesion between deposited particles, resuspension is also affected by TEP in the model through a time-varying critical shear stress (which is the threshold required to initiate erosion of the seabed and resuspension of mineral particles):

$$\tau_{cr}(t) = \tau_{cr}^{base} \times (1 + \delta_\tau \times \frac{[TEP]}{K_{TEP} + [TEP]})$$

where τ_{cr}^{base}= 0.1 Pa (base critical shear stress without TEP) and δ_τ= 2 (dimensionless enhancement factor). The multiplicative formulation reflects that TEP enhancement scales proportionally with baseline sediment properties, again with a saturation representing maximum biofilm stabilization capacity.

In response to the biologically-driven TEP effect on mineral particles, SPM affects phytoplankton growth through light attenuation (following a Beer-Lambert exponential attenuation as a function of depth with an attenuation coefficient as in Devlin et al., 2008), with potentially large effect on light availability at such SPM concentrations. The model was applied with realistic forcing (light, temperature, nutrients, tides) to simulate a typical year at MOW1. Results are shown in Figure 17. The model accurately simulates phytoplankton growth (carbon and Chl a; Fig.17a-b) with an initial spring bloom starting in February, depleting nutrients (especially P and Si; Fig.17d-e), followed by a second

extended summer bloom after remineralization of organic matter. TEP production and accumulation occurs during spring phytoplankton activity. Although TEP was not used for model calibration, its temporal evolution is well captured (Fig.17c), though concentrations appear underestimated (which may also be due to indirect observations and uncertain methodological conversion factors; see Fettweis et al., 2022). TEP increase drives floc diameter growth (Fig.17g), affecting settling velocity (Fig. 17h) and causing SPM concentration (Fig.17i) to decrease early in the year (as observed), then increase later as TEP decreases and resuspension exceeds settling. Notably, biologically-driven seasonal changes in floc diameter exceed physically-driven tidal fluctuations in magnitude (i.e., fast oscillations are smaller in amplitude than the seasonal evolution).

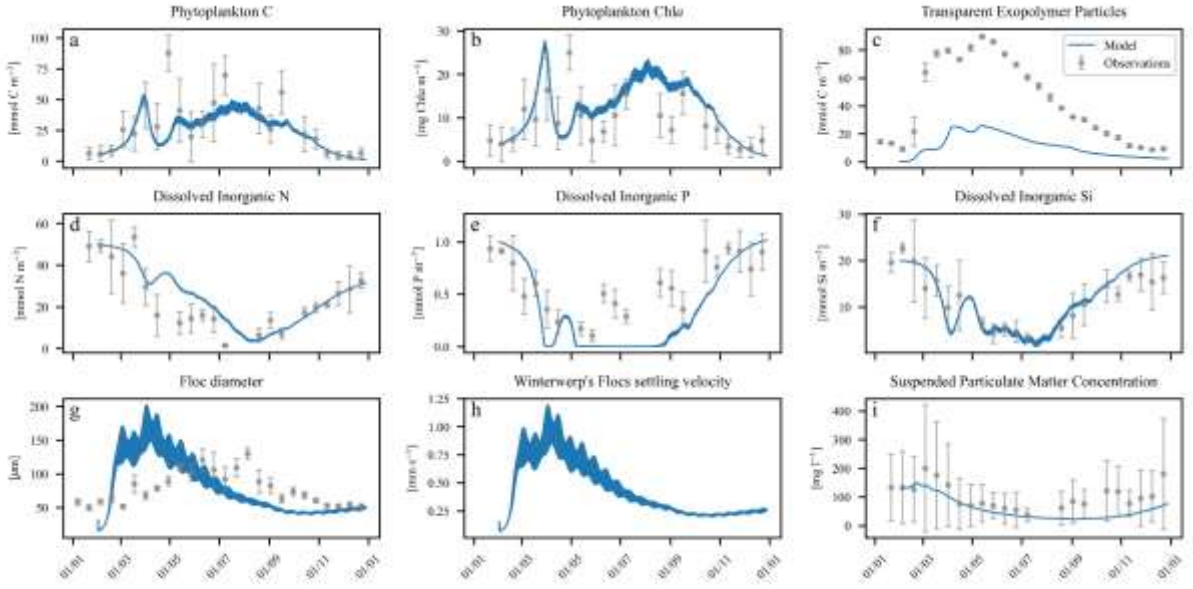

Figure 17 Seasonal evolution of simulated (blue lines) versus observed (grey symbols with standard deviation error bars) biogeochemical variables: (a-c) phytoplankton carbon, chlorophyll-a, and TEP concentrations, (d-f) dissolved inorganic nutrients (N, P, Si), (g-h) floc characteristics (diameter and settling velocity), and (i) suspended particulate matter. Units are provided in brackets for each variable.

Modeling tools enable "what-if" scenarios to test TEP effects on ecosystem dynamics by running equivalent simulations where TEP effects on SPM dynamics are cancelled (i.e., mineral flocculation uses only intrinsic baseline parameters without TEP-enhancement). Figure 18 shows comparisons between simulations with (blue) and without (orange) TEP effects on mineral flocs.

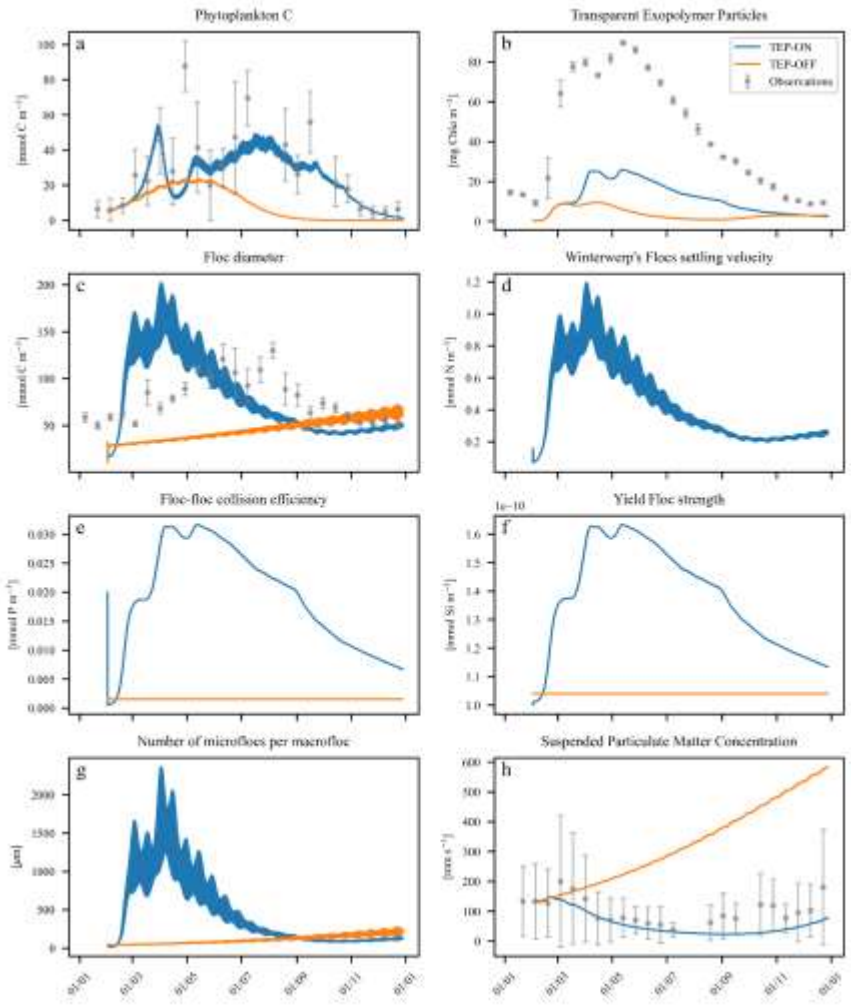

Figure 18 Comparison of seasonal dynamics between TEP-enabled (TEP-ON, blue) and TEP-disabled (TEP-OFF, orange) model simulations versus observations (grey symbols with standard deviation error bars): (a) phytoplankton carbon biomass, (b) TEP concentration, (c) floc diameter, (d) floc settling velocity, (e) collision efficiency, (f) floc yield strength, (g) number of microflocs per macrofloc, and (h) SPM concentration. Units are provided in brackets for each variable.

Without TEP effects, collision efficiency (Fig.18e) and floc strength (Fig.18f) remain constant at baseline levels, flocs stay small (Fig.18c-g), and SPM levels do not decrease seasonally, even increasing due to imbalanced resuspension. This significantly affects phytoplankton growth (Fig.18a): the spring bloom is impeded by insufficient light and never reaches reference levels, with the entire growing season affected by higher water column turbidity. Primary production is estimated to decrease by 6 to >90% depending on the month. Although the exact extent depends on model sensitivity to flocculation parameters (not shown), demonstrating the importance of feedback mechanisms between biological and mineral ecosystem components. These results suggest that phytoplankton modify their physical environment to overcome growth limitations, altering ecosystem functioning in turbid coastal waters and highlighting that organo-mineral interactions should become a higher priority in biogeochemical models.

The modeling results provide compelling evidence for the central hypotheses underlying BG-PART, and show that biological processes can fundamentally control suspended particulate matter dynamics in coastal turbid waters through complex feedback mechanisms. The successful representation of

multiple diatom species within a single modeling framework confirms that differences in light requirements and marine gel production capabilities can indeed drive seasonal phytoplankton succession and SPM dynamics. The model suggests that TEP-enhanced flocculation processes dominate over purely physical tidal forcing in determining seasonal patterns, supporting the concept that phytoplankton act as ecosystem engineers who actively modify their environment to overcome light limitations imposed by high turbidity. This biological control of the physical environment validates the hypothesis that early phytoplankton species shape conditions for subsequent primary production, creating a positive feedback loop that regulates habitability in naturally turbid coastal systems. The coupled biogeochemical-mineral flocculation model thus provides the first quantitative framework for understanding how organo-mineral interactions control ecosystem functioning in highly turbid coastal waters, establishing that accounting for these biological feedbacks should become a priority in coastal biogeochemical modeling studies, particularly given their potential importance for carbon sequestration and ecosystem services in productive coastal oceans.

Deliverables: The code of the coupled biogeochemical-mineral flocculation model is open source and available on GitHub under the European Union Public Licence (https://github.com/nterseleer/bgpartmod). Two peer-reviewed papers presenting the results of the laboratory experiments (Jourdevant et al., in prep.) and ecosystem applications (Terseleer et al., in prep.) are in development.

1.7. From space to sea, from particles to carbon cycle

1.7.1. Summary

The SPM, which concentration is observable from satellites and from in situ sampling, is a mixture of mineral and organic particles, which composition varies in space and time. Our semi-empirical model describing the POC content of SPM as a function of SPM concentration allows recalculating each component of POC from the SPM concentration. By combining satellite images of the surface SPM concentration in the North Sea, model data about stratification, and in situ data showing the vertical profiles of SPM concentration at many different locations, we can estimate the total mass of SPM in the water column of the North Sea. Thus, we can derive the total mass of POC and of its components with our semi-empirical model. Results show a total mass of POC in the North Sea roughly equal to 0.005 Pg C in winter and 0.001 Pg C in summer, composed mostly of the less reactive fractions of POC, POC_{slow} and POC_{min}. This mass of POC in suspension on the North Sea shelf is of the same order of magnitude as what is entering the North Sea and as what is buried in the shelf sediment each year.

1.7.2. The importance of shelf seas in the carbon cycle

Phytoplankton production on the North Sea shelf efficiently pumps atmospheric carbon dioxide, with the resulting biomass being remineralized beneath the pycnocline and exported as carbon dioxide to the North Atlantic, making the shelf a net carbon sink (Thomas et al., 2004; Laruelle et al., 2018; see Appendix Fig.A8). Only the Southern Bight of the North Sea, where the water column is continuously well mixed, constitutes on average a small source of carbon dioxide to the atmosphere, while the very nearshore zone should be a significant source because of terrestrial input (Thomas et al., 2004; Borges et al., 2005). There is consensus on the carbon dioxide balance on the North Sea shelf, but debate remains open on the fate of the organic carbon (de Haas et al., 2002). In the global ocean, phytoplankton production captures 50-75 x 10^{15} gC yr^{-1}, which, compared to a sediment burial rate of 0.16 × 10^{15} gC yr^{-1}, indicates an organic preservation efficiency in the marine environment of less than 0.5% (Hedges and Keil, 1995). This suggests that most of the organic carbon produced by phytoplankton and imported from lateral sources is remineralized in the water column, leading to relatively low carbon storage in sediments (Hedges et al., 1997). On the other hand, Hedges and Keil (1995) highlighted the importance of organic carbon associated with minerals in the carbon balance of the continental shelf seas. Organic components stabilized through their physical association with the mineral matrix of sediments form a fraction of reversibly linked organic molecules (Keil et al., 1994). This interaction stabilizes organic carbon, slowing or preventing further degradation, whether the organic matter is intrinsically labile or not (Hemingway et al., 2019; Kleber et al., 2021). Such organo-mineral association accounts for a major carbon sink in marine sediments. At the geological scale, this carbon preservation contributes to the atmospheric balance between oxygen and carbon dioxide that controls the climate (Hemingway et al., 2019). Shelf sea sediments are responsible for storing roughly 0.35 Pg C yr^{-1} worldwide, according to more recent estimates (Regnier et al., 2013; Keil, 2017), which corresponds to about 45% of preserved organic carbon in the global ocean (Yu et al., 2021). This highlights the important role of shelf seas in the global carbon cycle.

1.7.3. Combining satellite, in situ and model data

In this section our goal is to provide an estimate of the stock of fresh organic carbon, detritus organic carbon and mineral-associated organic carbon that can potentially be suspended in the water column of the North Sea shelf. This attempt requires several steps: using satellite products of daily surface SPM concentration to get a synoptic view of its variability in space and time; using model data to estimate the stratification regime of each considered pixel; using in situ data of vertical profiles of SPM

concentration to link surface concentrations to water column concentrations considering the stratification status; and applying our semi-empirical model to convert SPM to POC fractions (Fettweis et al., 2022; Silori et al., 2025a; see Appendix, Fig.A9).

While they are continuously subject to tidal settling and resuspension in well-mixed areas, particles obey different vertical distributions in the seasonally stratified areas of the shelf sea. In well-mixed waters, the vertical distribution of the SPM concentration can be seen as an exponential increasing toward the bottom and varying at tidal scale with current velocity (Fig.19). In thermally stratified waters (Fig.20), phytoplankton production takes place at the pycnocline (the lowest one in case of several levels of stratification), and the resulting POC settles in lower layers, while the shear stress on the sediment bed generates particle resuspension. The SPM concentration shows relatively low and vertically constant values in the surface mixed layer, increases progressively in the vicinity of the pycnocline, and shows relatively high and vertically constant values in deeper waters toward the bottom. The ratio between surface and bottom values can reach one order of magnitude in stratified areas like the Oysterground in the North Sea.

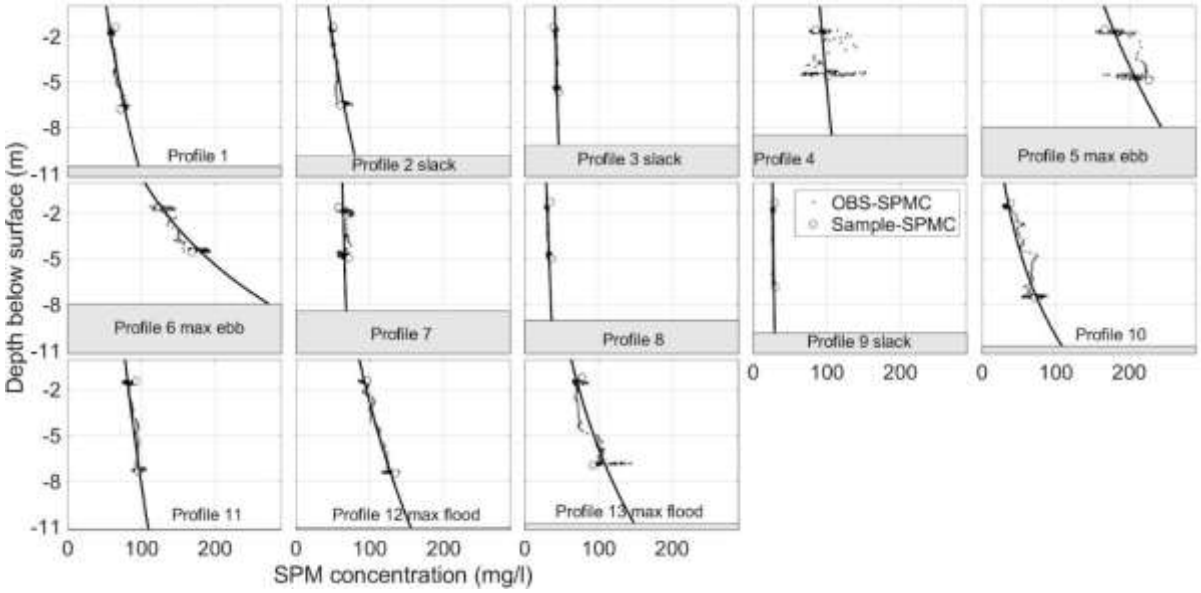

Figure 19 SPM concentration profile at the well-mixed station MOW1 (Belgian coastal zone) during a tidal cycle in November 2019 calculated from sample and OBS derived SPM concentration measurements.

Due to these difference in the vertical profiles of SPM concentration, the stratification regime of the water column needs to be considered if we want to establish a vertical integration of the SPM concentration on the North Sea shelf. The data collected by the R.V. Heincke in the period 2009-2010 across the German Bight (courtesy Rolf Riethmüller) offer vertical profiles of SPM concentration in many areas showing varying stratification regimes. These profiles were used to establish the ratio between the average SPM concentration in the water column and the surface SPM concentration (SPM_{mean}/SPM_{surf}). Probability distribution functions of that ratio (assumed unimodal and log normal) were made to extract median values of the ratio in each area and for each available month (Fig.21). Between year differences arise when the stratification is spatially extended, and this must be further analysed in the future to consider the impact of climate change on the stratification status and, thus, on the carbon cycle.

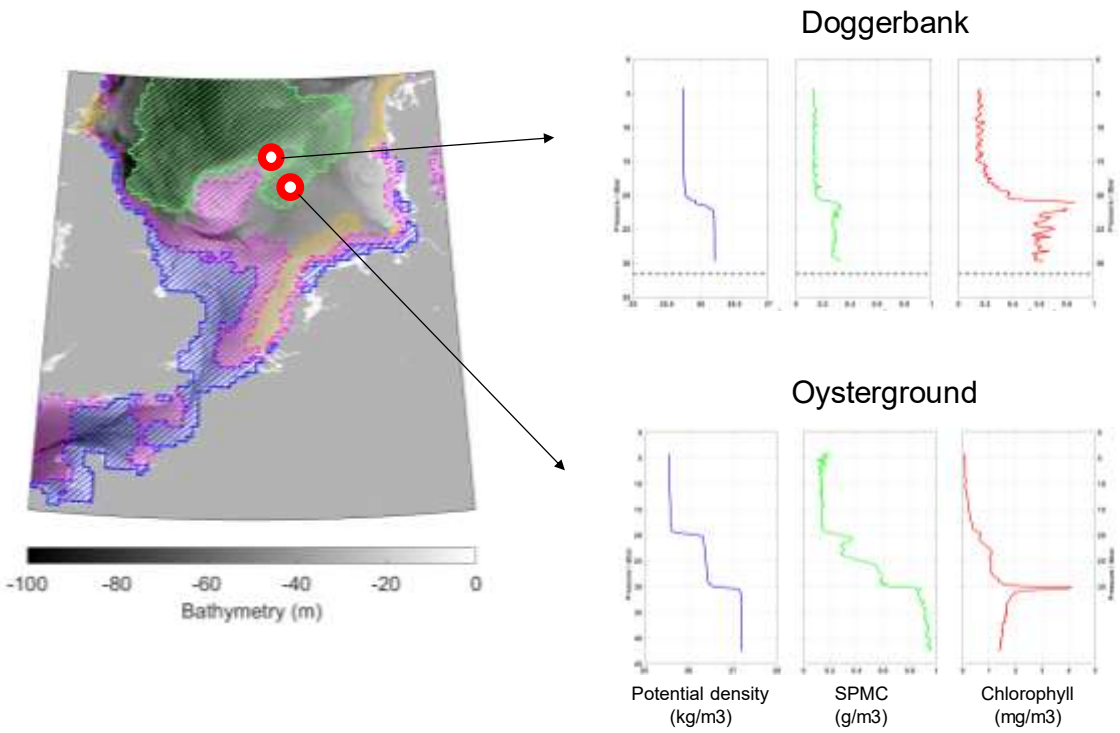

Figure 20 Left: Bathymetry of the North Sea with the representation of the different stratification regimes on average over 50 years of simulation (Van Leeuwen et al., 2015; blue, well-mixed; pink, intermittently stratified; green, seasonally stratified; yellow, ROFI). Right: Two stations along the trajectory of the R.V. Heincke have been selected to illustrate vertical profiles of the potential density, the SPM concentration and the chlorophyll concentration at two stratified stations with different stratification regimes in July 2010 (scanfish data, sampled on board the R.V. Heincke, period 2009-2013, courtesy of R. Riethmüller). Pressure indicates water depth (1 dbar ~ 1 m).

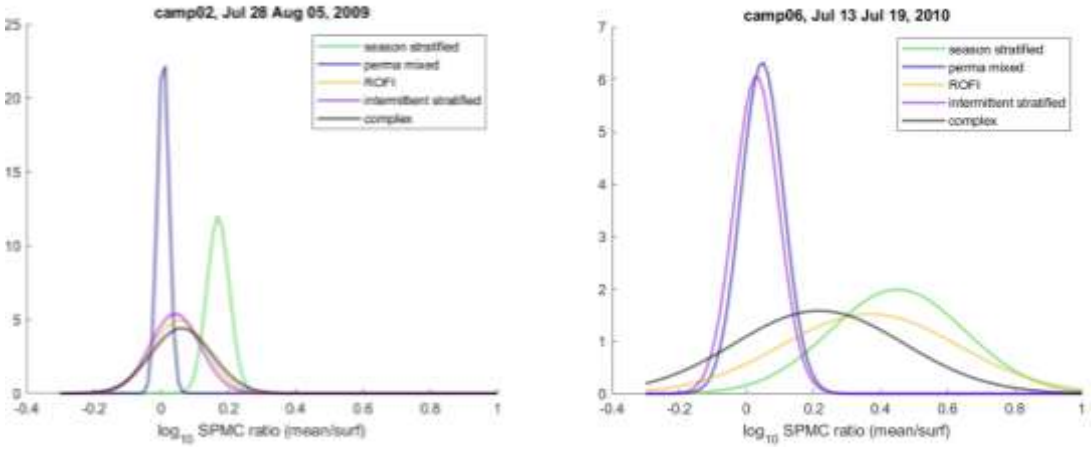

Figure 21 Probability density function (log-normal) calculated in each area showing a different stratification regime with the data sampled in situ (scanfish data, R.V. Heincke, courtesy of R. Riethmüller). The PDFs show the distribution of the ratio between the mean SPM concentration in the water column and the surface SPM concentration. Left: July 2009 with a 'normal' stratification. Right: July 2010 with a 'spatially extended' stratification.

The surface SPM concentration given by satellite products (courtesy D. Van der Zande) was then extrapolated vertically by using the mean ratio of SPM_{mean}/SPM_{surf} in each pixel considering the stratification status of the pixel at the moment. Combining that information with bathymetry, a vertically-integrated SPM could be calculated in each pixel for each season, converted into the corresponding vertically-integrated POC (Fig.22) with our semi-empirical model (Fettweis et al., 2022). The total POC in the water column of the North Sea shelf has been calculated together with the POC components (Fig.22, Table).

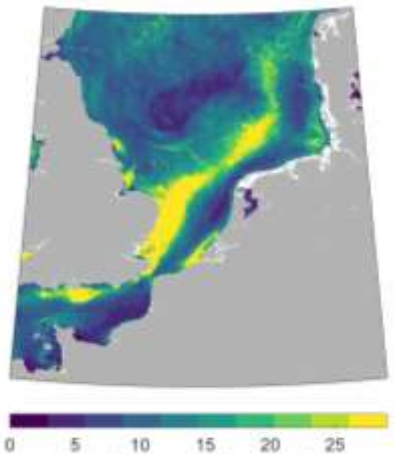

	Winter		Summer
POC	0,005 Pg C	- 88% →	0.0011 Pg C
$POC_{min/slow}$	100%		80%
POC_{fresh}	<1%		20%

Figure 22 Left: Recalculated map showing the vertically integrated POC in winter (units: g C m^{-2}). Right: Table showing the total mass of POC in the water column of the North Sea shelf (covered domain is shown on the map) in winter and in summer. The percentage composition (in mass) of both reactive (POC_{fresh}) and less reactive (POC_{min}+POC_{slow}) components is also shown for each season.

Based on previous works estimating the SPM loads from rivers entering the North Sea and the erosion of Suffolk and Holderness (Dobrynin, 2009), and the SPM net flux entering from the Channel (Fettweis et al., 2007), we estimated the total SPM flux entering the North Sea equal to ~40 10^6 ton yr^{-1}. This amount roughly corresponds to a flux of 0.001 Pg C yr^{-1} of mineral-associated POC and detritus POC (the less reactive fractions of POC). We also estimated the flux of organic carbon deposited in the sediment of the North Sea from the values provided by Regnier et al. (2013) and Keil (2017). Adapted to the surface of the North Sea considered in Fig.22, the flux of carbon deposited in the sediment is approximately 0.006 Pg C yr^{-1}. In this study, we calculated the winter amount of mineral-associated POC and detritus POC in suspension on the North Sea shelf to be equal to 0.005 Pg C (0.001 Pg C in summer). We conclude that the particulate organic carbon in suspension in the water column of the North Sea exhibits a total mass of the same order of magnitude as what is entering the North Sea and as what is buried in the shelf sediment each year. This assessment is a basis for future estimates of the carbon budget on productive shelf systems. It is recongnized that carbon cycle budgets and fluxes are poorly constrained due, for instance, to the uncertainty on observed data or the difficulty to extrapolate local observations at the global scale. This study focusing on stock estimates on the basis of satellite images and in situ samplings also aims at constraining better the carbon budgets on shelf seas with the synoptic and high resolution remote sensing observations.

2. General conclusions

Phytoplankton seldom finds optimal growth condition in turbid waters like in the Belgian coastal zone. Nevertheless, the phytoplankton community is able to start photosynthesis at the end of the winter despite higher SPM concentration on average. Winter-spring phytoplankton communities may be very different from year to year, especially when the winter temperature differs. Although the conditions by which the onset of the bloom takes place are not fully elucidated, we hypothesize that phytoplankton attached to particle – usually benthic species acquainted to low light conditions – can make photosynthesis while particles are resuspended during the tide. Also, photosynthesis is improved when particle settle down during the tidal cycle while phytoplankton cells and colonies remain closer to the surface by differential settling, as shown by the vertical distribution of chlorophyll concentration and of the POC content of SPM (Silori et al., 2025b). Like in the open ocean, coastal phytoplankton communities produce marine gels and their precursors (EPS). EPS and TEP production is ubiquitous, except in *Phaeocystis globosa*, while smaller phytoplankton cells have generally a higher capacity for the production of EPS and TEP. The presence of phytoplankton and EPS enhance the flocculation of suspended particles as shown by lab experiments, which supports the hypothesis of Fettweis et al. (2022) that the seasonal decrease in the SPM concentration is explained by the accumulation of freshly produced TEP in spring and summer. This biological control of the physical environment is also reproduced by our 0D model, which validates the hypothesis that early phytoplankton species shape conditions for subsequent primary production, creating a positive feedback loop that regulates habitability in naturally turbid coastal systems. Indeed, such seasonal variation of the SPM concentration by marine gels has in turn a substantial impact on phytoplankton production, as shown by the 0D model outcome. This particle dynamics in the vertical also modulates the horizontal transport of particles, especially across the coastal-offshore gradient. We have observed that the concentration of particles (organic and mineral) tend to decrease from the coast to the offshore, especially at bathymetries below 20 m on average. Presumably, in that transition zone, the turbulence range and particle composition favor particle settling, while hydrodynamic processes tend to transport particles of the seabed back towards the coast, thus maintaining the cross-shore SPM gradient. As particle dynamics play a substantial role in biogeochemical fluxes, we have extended these concepts to the whole North Sea by combining satellite images, hydrodynamic model results and in situ data to contribute assessing the carbon budget on the shelf.

We recommend to conduct future research in this domain in an attempt to elucidate what we could not address in BG-PART. More specifically, some questions are:

- It is as yet unclear how EPS, TEP and phytoplankton interact to enhance the flocculation of particles. Is EPS, in the form of DOC or colloids, sufficient to strengthen the cohesion between encountering particles in a turbid system? Or is TEP needed as it occurs in the open ocean?
- The 0D box model can be extended progressively to a 1D vertical and then to a 3D model. This would help to better resolve the spatial complexity (vertical and horizontal) of organo-mineral particle dynamics and transport across gradients.
- To explain the sorptive interactions between dissolved organic carbon and mineral particles, one may analyse the nature of dissolved organic molecules, and also their origin. This would help to understand better the coastal carbon fluxes.
- To improve the carbon budget on the North Sea shelf, we may study the fate of the incoming suspended organic carbon from erosion, rivers and ocean source. Does it vary on the long term? Is it transported away, or does it deposit in the bottom sediment or in intertidal areas?

3. Valorization

3.1. Publications in scientific journals

1. Desmit, X., Schartau, M., Riethmüller, R., Terseleer, N., Van der Zande, D., Fettweis, M., **2024**. The transition between coastal and offshore areas in the North Sea unraveled by suspended particle composition. Science of The Total Environment 915, 169966. https://doi.org/10.1016/j.scitotenv.2024.169966
2. Fettweis, M., Silori, S., Adriaens, R., Desmit, X., **2025**. Clay minerals and the stability of organic carbon in suspension along coastal to offshore transects. Geochimica et Cosmochimica Acta 395, 229–237. https://doi.org/10.1016/j.gca.2025.03.003
3. Fettweis, M., Belliard, J.-P., Silori, S., Terseleer, N., Tran, D., Amadei Martinez, L., Brun, A., Sabbe, K., De Rijcke, M., Lee, B.J., Riethmüller, R., Shen, X., Verney, R., Desmit, X., **in.rev.** Suspended particulate matter along the land-ocean continuum. Submitted to Nature Review.

3.2. PhD defense

Dr. Auria Loïse Brun was fully paid on the BG-PART project to conduct a PhD in biological sciences at the PAE laboratory of Ghent University, and she successfully defended her thesis on November 18, 2025.

Brun, A., **2025**. Deciphering the role of phytoplankton and their production of marine gels in suspended particulate matter dynamics in the Belgian Part of the North Sea. PhD thesis, Ghent University. Promotor: Prof. Dr. Koen Sabbe. Co-promotors: Dr. Dimitra-Ioli Skouroliakou and Dr. Xavier Desmit

3.3. Workshop on Pelagic Particle Dynamics

The Workshop was held in October 4-6, **2023** at RBINS, Vautier Street 29, 1000 Brussels. A manuscript summarizing our discussions has been submitted and is under revision (see Valorization, Publications).

3.4. International conferences

1. Kallend, A., Dujardin, J.H., Fettweis, M., Vyverman, W., De Rijcke, M., Sabbe, K., Desmit, X., **2023**. Interactions between phytoplankton, marine gels and suspended particulate matter in a dynamic, shallow coastal system before and during the phytoplankton spring bloom (Poster). Presented at the ASLO Aquatic Sciences Meeting, 4-9 Jun, Palma De Mallorca, Spain.
2. Kallend, A., Amadei Martinez, L., Debusschere, M., Skouroliakou, D.-I., Fettweis, M., Desmit, X., Vyverman, W., Sabbe, K., **2024**. Light-temperature niche in North Sea phytoplankton : Potential implications of changing environment pressures on phytoplankton seasonal succession and marine gels production. Presented at the 57th European Marine Biology Symposium (EMBS), 16-20 Sep, Naples, Italy.
3. Terseleer, N., Fettweis, M., Silori, S., Desmit, X., Kallend, A., Amadei Martinez, L., Sabbe, K., Vyverman, W., Lee, B.J., Kerimoglu, O., **2024**. A coupled phytoplankton-flocculation model to quantify suspended particulate matter dynamics on the Belgian shelf. Presented at the AMEMR 2024 Conference, 8-11 July, Plymouth, UK.
4. Desmit, X., Riethmüeller, R., Silori, S., Van der Zande, D., Schartau, M., Fettweis, M., **2025**. Budgeting the particulate organic matter from the suspended particulate matter in shelf seas. Presented at the EGU25 Conference, Session BG4.2, April 30, Vienna, Austria.

4. Follow-Up Committee

The Follow-Up Committee has been of great help during the project. Not only they guided us from the start, including by participating to the Workshop we organized halfway through the project, but they are also involved as co-authors in published and submitted papers, as well as in papers in preparation. We would like to warmly thank each member of the Follow-Up Committee for their contributions and support.

5. Problems and Solutions

1. Despite the R.V. Belgica being out of service between summer 2024 and winter 2025, we are pleased to announce that our consortium made full use of its availability. Between 2022 and 2024, our consortium conducted 15 campaigns aboard the R.V. Belgica and 2 campaigns aboard the R.V. Simon Stevin. This allowed collecting 760 water samples using rosettes, from which numerous parameters were measured. We thank the MSO and ECOCHEM teams at RBINS, the staff at UGent and VLIZ for their support with the analyses, as well as the crews of the R.V. Belgica and the R.V. Simon Stevin.

2. A significant portion (20%) of the budget initially allocated to RBINS staff salaries for the BG-PART project was withdrawn by RBINS management. As a result, we were unable to finalize certain tasks, including some of the necessary transdisciplinary discussions within the BG-PART project context once all the data had been collected. We nevertheless plan to organize discussions in the coming months and disseminate some findings that have not yet been published.

Literature

Amadei Martínez, L., Sabbe, K., Fettweis, M., Desmit, X., Israel, Y., Bakker, W., Dasseville, R., D'hondt, S., Daveloose, I., Verstraete, T., Chaerle, P., Brion, N., Maris, T., Vyverman, W., 2025. Phytoplankton enhances the flocculation of suspended particulate matter in a turbid estuary. Limnol. Oceanogr. 70, 3431–3446. https://doi.org/10.1002/lno.70216

Anderson, T.R., Christian, J.R., Flynn, K.J., 2015. Modeling DOM biogeochemistry, in: Hansell, D.A., Carlson, C.A. (Eds.), Biogeochemistry of Marine Dissolved Organic Matter (Second Edition). Academic Press, Boston, pp. 635–667. https://doi.org/10.1016/B978-0-12-405940-5.00015-7

Arndt, S., Jørgensen, B.B., LaRowe, D.E., Middelburg, J.J., Pancost, R.D., Regnier, P., 2013. Quantifying the degradation of organic matter in marine sediments: A review and synthesis. Earth-Sci. Rev. 123, 53–86. https://doi.org/10.1016/j.earscirev.2013.02.008

Borges, A.V., Delille, B., Frankignoulle, M., 2005. Budgeting sinks and sources of CO2 in the coastal ocean: Diversity of ecosystems counts. Geophys. Res. Lett. 32. https://doi.org/10.1029/2005GL023053

de Haas, H., van Weering, T.C.E., de Stigter, H., 2002. Organic carbon in shelf seas: sinks or sources, processes and products. Cont. Shelf Res. 22, 691–717. https://doi.org/10.1016/S0278-4343(01)00093-0

Desmit, X., Schartau, M., Riethmüller, R., Terseleer, N., Van der Zande, D., Fettweis, M., 2024. The transition between coastal and offshore areas in the North Sea unraveled by suspended particle composition. Sci. Total Environ. 915, 169966. https://doi.org/10.1016/j.scitotenv.2024.169966

Devlin, M.J., Barry, J., Mills, D.K., Gowen, R.J., Foden, J., Sivyer, D., Tett, P., 2008. Relationships between suspended particulate material, light attenuation and Secchi depth in UK marine waters. Estuar. Coast. Shelf Sci. 79, 429–439. https://doi.org/10.1016/j.ecss.2008.04.024

Dobrynin, M., 2009. Investigating the dynamics of suspended particulate matter in the North Sea using a hydrodynamic transport model and satellite data assimilation. Hamburg University, Hamburg. ISSN 0344-9629. https://www.hereon.de/imperia/md/content/hzg/zentrale_einrichtungen/bibliothek/berichte/2009/gkss_2009_12.pdf.

Engel, A., Endres, S., Galgani, L., Schartau, M., 2020. Marvelous Marine Microgels: On the Distribution and Impact of Gel-Like Particles in the Oceanic Water-Column. Front. Mar. Sci. 7. https://doi.org/10.3389/fmars.2020.00405

Engel, A., Thoms, S., Riebesell, U., Rochelle-Newall, E., Zondervan, I., 2004. Polysaccharide aggregation as a potential sink of marine dissolved organic carbon. Nature 428, 929–932. https://doi.org/10.1038/nature02453

Fettweis, M., Nechad, B., Van den Eynde, D., 2007. An estimate of the suspended particulate matter (SPM) transport in the southern North Sea using SeaWiFS images, in situ measurements and numerical model results. Cont. Shelf Res. 27, 1568–1583. https://doi.org/10.1016/j.csr.2007.01.017

Fettweis, M., Schartau, M., Desmit, X., Lee, B.J., Terseleer, N., Van der Zande, D., Parmentier, K., Riethmüller, R., 2022. Organic Matter Composition of Biomineral Flocs and Its Influence on Suspended Particulate Matter Dynamics Along a Nearshore to Offshore Transect. J. Geophys. Res. Biogeosciences 127, e2021JG006332. https://doi.org/10.1029/2021JG006332

Fettweis, M., Silori, S., Adriaens, R., Desmit, X., 2025. Clay minerals and the stability of organic carbon in suspension along coastal to offshore transects. Geochim. Cosmochim. Acta 395, 229–237. https://doi.org/10.1016/j.gca.2025.03.003

Hedges, J.I., Keil, R.G., 1995. Sedimentary organic matter preservation: an assessment and speculative synthesis. Mar. Chem. 49, 81–115. https://doi.org/10.1016/0304-4203(95)00008-F

Hedges, J.I., Keil, R.G., Benner, R., 1997. What happens to terrestrial organic matter in the ocean? Org. Geochem. 27, 195–212. https://doi.org/10.1016/S0146-6380(97)00066-1

Hemingway, J.D., Rothman, D.H., Grant, K.E., Rosengard, S.Z., Eglinton, T.I., Derry, L.A., Galy, V.V., 2019. Mineral protection regulates long-term global preservation of natural organic carbon. Nature 570, 228–231. https://doi.org/10.1038/s41586-019-1280-6

Ho, Q.N., Fettweis, M., Spencer, K.L., Lee, B.J., 2022. Flocculation with heterogeneous composition in water environments: A review. Water Res. 213, 118147. https://doi.org/10.1016/j.watres.2022.118147

Keil, R., 2017. Anthropogenic Forcing of Carbonate and Organic Carbon Preservation in Marine Sediments. Annu. Rev. Mar. Sci. 9, 151–172. https://doi.org/10.1146/annurev-marine-010816-060724

Keil, R.G., Mayer, L.M., 2014. Mineral Matrices and Organic Matter, in: Holland, H.D., Turekian, K.K. (Eds.), Treatise on Geochemistry (Second Edition). Elsevier, Oxford, pp. 337–359. https://doi.org/10.1016/B978-0-08-095975-7.01024-X

Keil, R.G., Montluçon, D.B., Prahl, F.G., Hedges, J.I., 1994. Sorptive preservation of labile organic matter in marine sediments. Nature 370, 549–552. https://doi.org/10.1038/370549a0

Kerimoglu, O., Hintz, N.H., Lücken, L., Blasius, B., Böttcher, L., Bunse, C., Dittmar, T., Heyerhoff, B., Mori, C., Striebel, M., Simon, M., 2022. Growth, organic matter release, aggregation and recycling during a diatom bloom: A model-based analysis of a mesocosm experiment. https://doi.org/10.1101/2022.05.18.492269

Kleber, M., Bourg, I.C., Coward, E.K., Hansel, C.M., Myneni, S.C.B., Nunan, N., 2021. Dynamic interactions at the mineral–organic matter interface. Nat. Rev. Earth Environ. 2, 402–421. https://doi.org/10.1038/s43017-021-00162-y

Laruelle, G.G., Cai, W.-J., Hu, X., Gruber, N., Mackenzie, F.T., Regnier, P., 2018. Continental shelves as a variable but increasing global sink for atmospheric carbon dioxide. Nat. Commun. 9, 454. https://doi.org/10.1038/s41467-017-02738-z

Lee, B.J., Toorman, E., Molz, F.J., Wang, J., 2011. A two-class population balance equation yielding bimodal flocculation of marine or estuarine sediments. Water Res. 45, 2131–2145. https://doi.org/10.1016/j.watres.2010.12.028

Maerz, J., Hofmeister, R., van der Lee, E.M., Gräwe, U., Riethmüller, R., Wirtz, K.W., 2016. Maximum sinking velocities of suspended particulate matter in a coastal transition zone. Biogeosciences 13, 4863–4876. https://doi.org/10.5194/bg-13-4863-2016

Postma, H., 1984. Introduction to the symposium on organic matter in the Wadden Sea. Neth Inst Sea Res - Publ. Ser. 10, 15–22.

Quigg, A., Santschi, P.H., Burd, A., Chin, W.-C., Kamalanathan, M., Xu, C., Ziervogel, K., 2021. From Nano-Gels to Marine Snow: A Synthesis of Gel Formation Processes and Modeling Efforts Involved with Particle Flux in the Ocean. Gels 7, 114. https://doi.org/10.3390/gels7030114

Regnier, P., Friedlingstein, P., Ciais, P., Mackenzie, F.T., Gruber, N., Janssens, I.A., Laruelle, G.G., Lauerwald, R., Luyssaert, S., Andersson, A.J., Arndt, S., Arnosti, C., Borges, A.V., Dale, A.W., Gallego-Sala, A., Goddéris, Y., Goossens, N., Hartmann, J., Heinze, C., Ilyina, T., Joos, F., LaRowe, D.E., Leifeld, J., Meysman, F.J.R., Munhoven, G., Raymond, P.A., Spahni, R., Suntharalingam, P., Thullner, M., 2013. Anthropogenic perturbation of the carbon fluxes from land to ocean. Nat. Geosci. 6, 597–607. https://doi.org/10.1038/ngeo1830

Sarthou, G., Timmermans, K.R., Blain, S., Tréguer, P., 2005. Growth physiology and fate of diatoms in the ocean: a review. J. Sea Res., Iron Resources and Oceanic Nutrients - Advancement of Global Environmental Simulations 53, 25–42. https://doi.org/10.1016/j.seares.2004.01.007

Schartau, M., Riethmüller, R., Flöser, G., van Beusekom, J.E.E., Krasemann, H., Hofmeister, R., Wirtz, K., 2019. On the separation between inorganic and organic fractions of suspended matter in a marine coastal environment. Prog. Oceanogr. 171, 231–250. https://doi.org/10.1016/j.pocean.2018.12.011

Silori, S., Desmit, X., Fettweis, M., 2025a. Spatio-temporal variation in particulate and dissolved organic matter dynamics in the southern North Sea. Biogeochemistry 168, 96. https://doi.org/10.1007/s10533-025-01288-7

Silori, S., Desmit, X., Riethmüller, R., Schartau, M., Terseleer, N., Fettweis, M., 2025b. Vertical dynamics of suspended particulate matter and chlorophyll-a in a well-mixed coastal turbid system. Estuar. Coast. Shelf Sci. 109545. https://doi.org/10.1016/j.ecss.2025.109545

Terseleer, N., Bruggeman, J., Lancelot, C., Gypens, N., 2014. Trait-based representation of diatom functional diversity in a plankton functional type model of the eutrophied southern North Sea. Limnol. Oceanogr. 59, 1958–1972. https://doi.org/10.4319/lo.2014.59.6.1958

Thomas, H., Bozec, Y., Elkalay, K., de Baar, H.J.W., 2004. Enhanced Open Ocean Storage of CO2 from Shelf Sea Pumping. Science 304, 1005–1008. https://doi.org/10.1126/science.1095491

van Leeuwen, S., Tett, P., Mills, D., van der Molen, J., 2015. Stratified and nonstratified areas in the North Sea: Long-term variability and biological and policy implications. J. Geophys. Res. Oceans 120, 4670–4686. https://doi.org/10.1002/2014JC010485

Yu, M., Eglinton, T.I., Haghipour, N., Montluçon, D.B., Wacker, L., Hou, P., Ding, Y., Zhao, M., 2021. Contrasting fates of terrestrial organic carbon pools in marginal sea sediments. Geochim. Cosmochim. Acta 309, 16–30. https://doi.org/10.1016/j.gca.2021.06.018

APPENDIX: Summary of the project

To provide an overview of the different aspects of the BG-PART project – hydrodynamics, sedimentology, biology and biogeochemistry – we present some of our results in the form of a synthesis illustrated by some of the graphical abstracts we have produced in our scientific publications and conference communications.

5.1. Suspended particle composition in the marine system

Minerals and organic matter (OM) are the major constituents of suspended particulate matter (SPM) in aquatic systems. Marine OM constitutes a mixture of plankton (phytoplankton, bacteria, etc.), exudates, detritus, fecal pellets, organic molecules originating from diverse autochthonous and allochthonous sources and organo-mineral associations (Arndt et al., 2013; Keil and Mayer, 2014). The particulate organic carbon (POC) is made of living cells, detritus and organic carbon adsorbed on mineral surfaces (Fig.A1), all of which follow very different biogeochemical pathways.

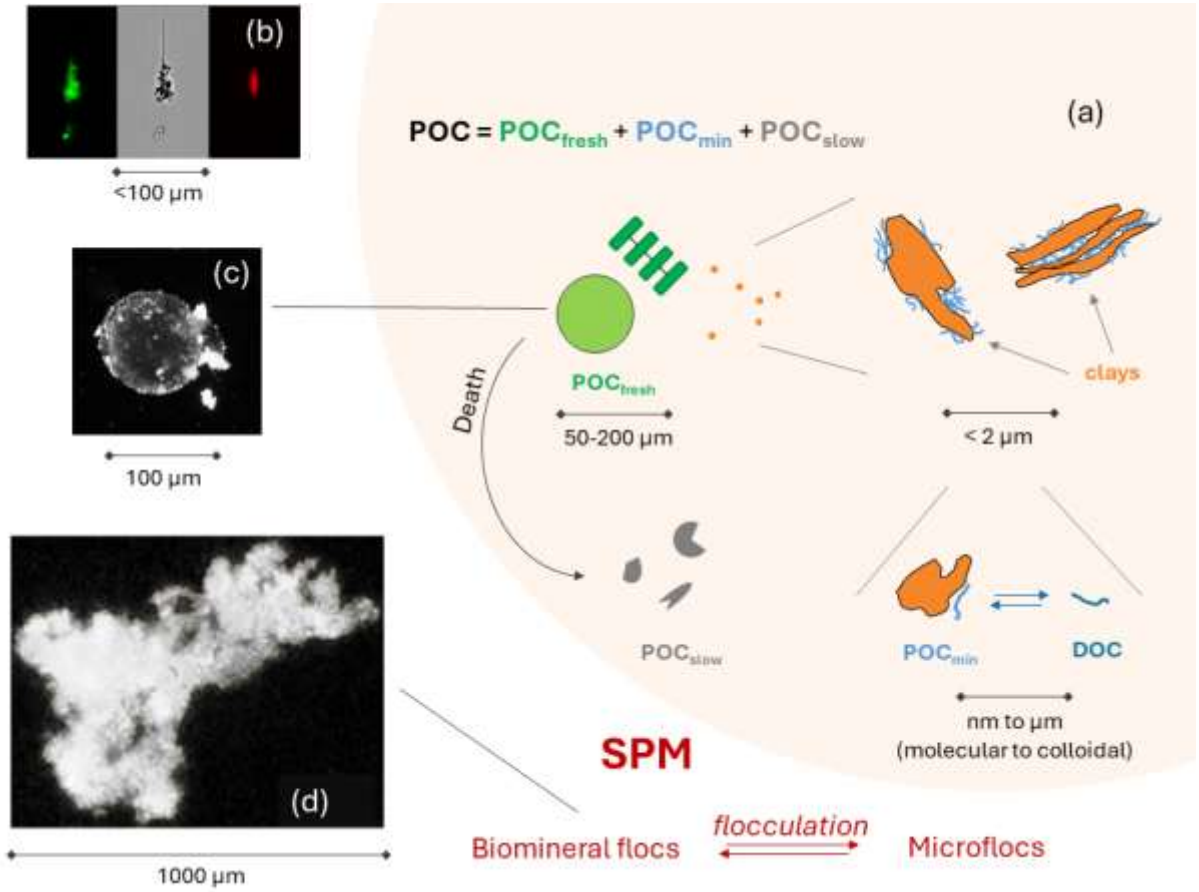

Figure A1 SPM composition in the marine system. (a) Schematic representation of primary particles featuring the clay particles and the different fractions of particulate organic carbon (POC). POC is the sum of its fractions: the reactive fraction POC_{fresh}, the less reactive detritic fraction POC_{slow}, and the less reactive mineral-associated POC_{min}, the latter being the product of sorptive interactions between the mineral surface of clay particles and the dissolved organic carbon (DOC). (b) Image of a particle attached with a phytoplankton cell smaller than 100 µm obtained with imaging Flow Cytometry (iFCM; courtesy PAE, Ugent), with DNA material in green and chloroplast material in red. (c) In situ picture of a spherical particle with smaller particles sticking at its surface made with the Particle Camera (PCam) in the water column of the Belgian coastal zone (courtesy L. Delhaye).

Image analysis is under work to confirm whether the particle is a phytoplankton cell. (d) In situ picture of a large biomineral floc with complex non-spherical shape made with the PCam in the Belgian coastal zone (courtesy L. Delhaye). The biomineral flocs are a transient product of the aggregation of smaller particles during the flocculation process (aggregation and disaggregation) continuously occurring during the tidal cycle.

Mineral particles in suspension are mainly composed of clays, carbonates, quartz and opal (Fettweis et al., 2025), of which clays are particularly cohesive and flocculate under natural conditions. The horizontal transport of particles depends on their vertical dynamics, which directly relies on their composition (mineral, living, detritic...). The organic content of SPM (the POC content) varies with the SPM concentration, notably along its cross-shore gradient (Fig.A2a), with a dominance of POC_{fresh} at low SPM concentration and of POC_{min}+POC_{slow} at high SPM concentration. More generally, the composition of SPM depends on multiple interacting factors (Fig.A2b). The complex nature and dynamics of suspended particles in the natural system of the North Sea imposes the deployment of many different techniques of observation to capture meaningful information on SPM (see Fig.A4).

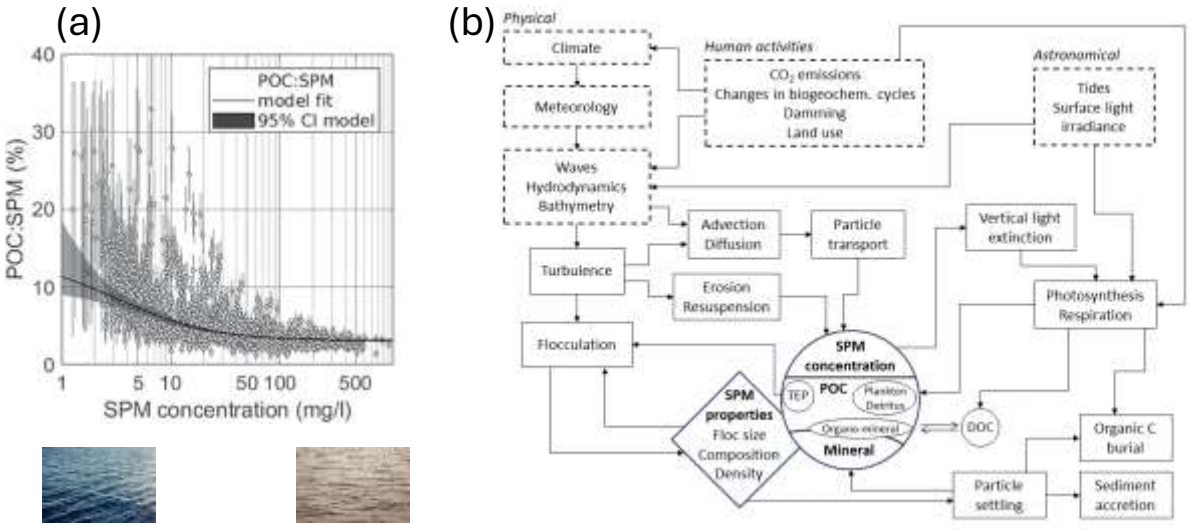

Figure A2 (a) Variation of the POC content of SPM as a function of the SPM concentration. (b) Processes affecting the dynamics and biogeochemistry of SPM. Arrows mean 'has an influence on'; external drivers are framed with dashed lines, processes are framed with rectangles, and concentrations with rounded shapes.

5.2. Seasonal variability in SPM concentration

Clay particles flocculate naturally to form small flocs. Because phytoplankton exudates exopolymeric substances (EPS) during photosynthesis, even in a turbid and eutrophied system like the Belgian coastal zone, it influences the particle dynamics. These freshly produced EPS can aggregate to form larger transparent exopolymeric particles (TEP, Engel et al., 2004), which sticky properties are assumed to enhance flocculation (Fettweis et al., 2022; Fig.A3). Under varying turbulence conditions, mineral and organic particles collide and aggregate in larger biomineral flocs or disaggregate in microflocs, releasing living and detritic components. These flocs may settle down to the seabed when their size reaches sufficiently high values to allow breaking the viscosity of water while current velocities decrease, and may in turn be resuspended from the sediment bed by turbulent shear stress when current velocities increase. Hence, the tide and wind driven turbulence continuously induces a change in particle size and composition, and redistributes particles in the water column at hourly scale.

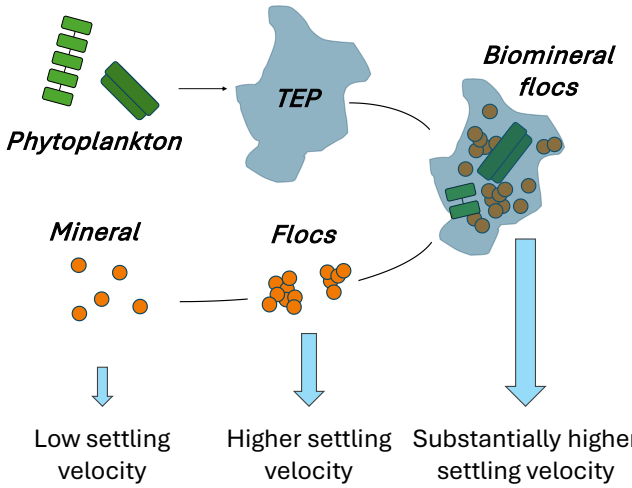

Figure A3 The byproduct exudates of phytoplankton photosynthesis aggregate to form sticky TEP that will enhance the flocculation of particles and the formation of larger biomineral flocs. With larger sizes on average in summer, flocs will also have a larger settling velocity as they are less affected by the viscosity of water.

As phytoplankton photosynthesis accumulates fresh TEP in the water column, flocs tend to get a larger median size in the summer which increases their settling velocities toward the bottom. On average over a tidal cycle, particles thus spend more time closer to the bottom in the summer than in the winter, which is observed as a seasonal decrease in the SPM concentration in the summer (Fig.A4).

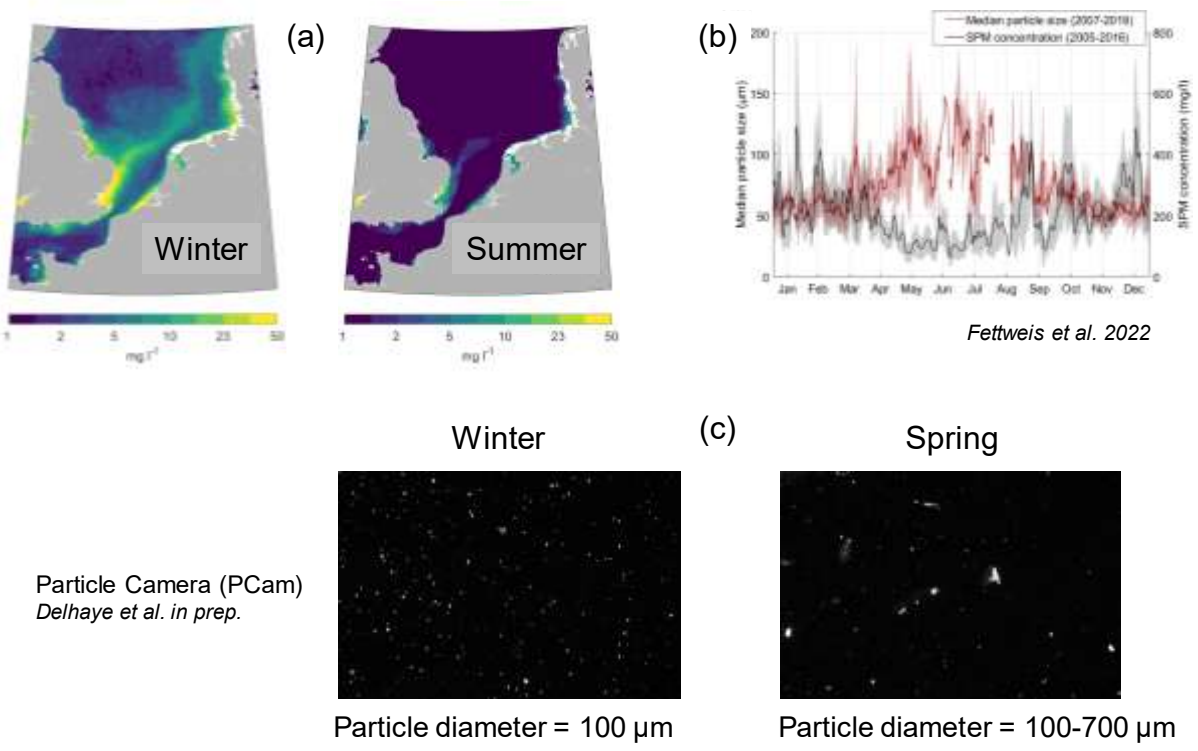

Figure A4 Illustration of the seasonal varibility in the SPM concentration in the North Sea. (a) Satellite product of surface SPM concentration in winter and in summer showing the ubiquitous seasonal decrease in SPM concentration. (b) Continuous time series of both the SPM concentration (black) and the median particle size (red) at station MOW1 in the turbid Belgian coastal zone. (c) PCam images of numerous and small particles in the winter and of less numerous particles with a larger size spectrum in the summer in Belgian coastal waters.

5.3. Spatial variability in SPM concentration

In most turbid coastal zones of the North Sea and the Channel, where adjacent freshwater is discharged at river outlets (such as in the Belgian coastal zone, the German Bight or the Bay of Seine), particles are subject to a trapping mechanism that tends to keep them at the coast (Fig.A5; see also Maerz et al., 2016).

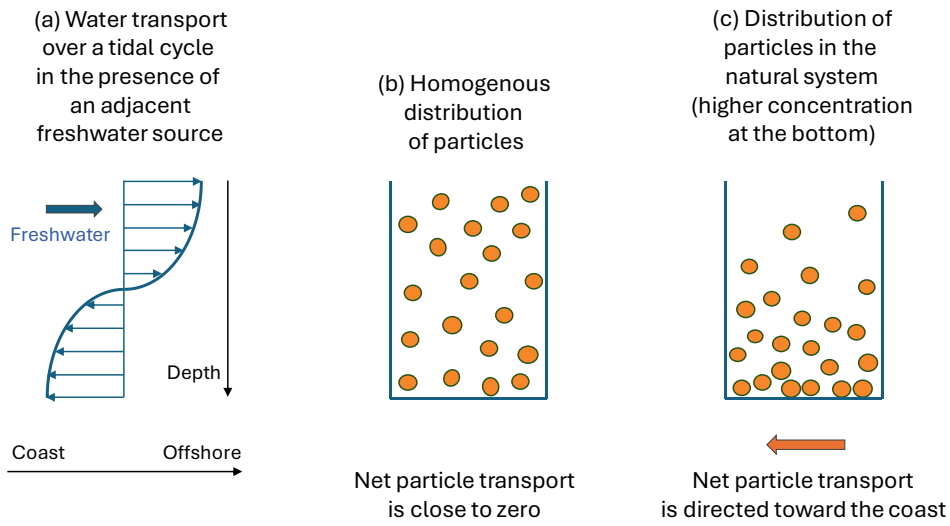

Figure A5 The input of freshwater to a coastal area influences the vertical distribution of water transport during tides, even in the absence of stratification, and thus the transport of particles. (a) During a complete tidal cycle (flood and ebb), bottom water is transported slightly more towards the coast than surface water. (b) This vertical distribution would have little impact on particle transport if particles were homogeneously distributed throughout the water column. (c) However, in the natural system, particles exhibit a vertical distribution with higher concentrations at the bottom. Therefore, even in the hypothetical case where the net water transport were zero over a tidal cycle and across the vertical – as shown in (a) –, the difference in water transport between the surface and the bottom during flood and ebb would result in a net transport of particles towards the shore.

This mechanism is reinforced by enhanced flocculation as is the case in the spring and the summer when phytoplankton produces EPS/TEP. Under this effect, most coastal particles tend to remain in the transition zone that extends from the coast to the offshore at bathymetries below 20 metres (Fig.A6; Desmit et al., 2024). As particle dynamics have a substantial influence on biogeochemical processes, we propose that this mechanism, when applicable, can be used to distinguish coastal from offshore waters.

Beside crosh-shore gradients in SPM concentration and composition, the vertical distribution of SPM concentration varies substantially from well-mixed areas to seasonally stratified areas. While SPM concentration obeys an exponential increase toward the bottom in well mixed areas, it follows different profiles in stratified waters, especially it can exhibit concentrations below the pycnocline ten times higher than above the pycnocline (see, e.g., Fig.A8b).

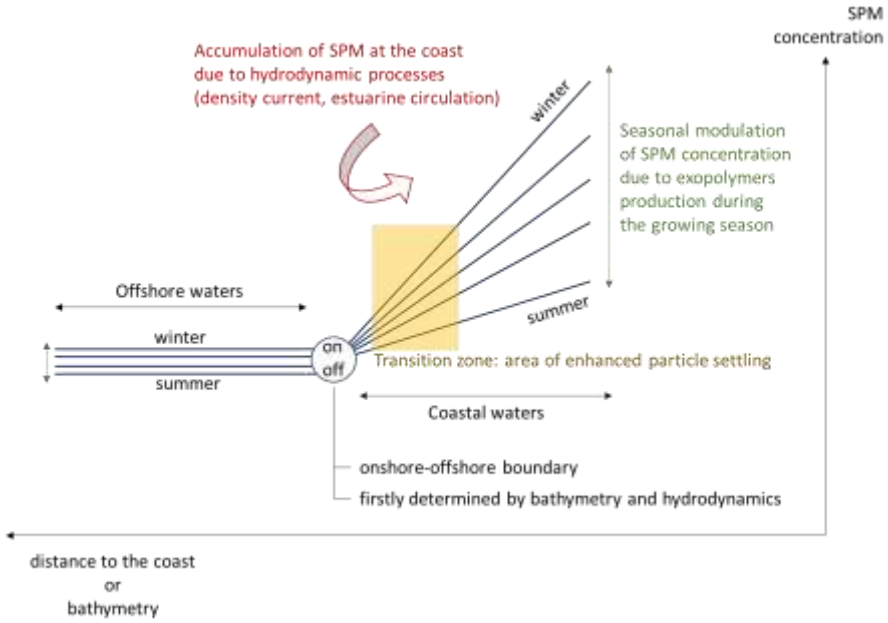

Figure A6 Scheme describing the distinction between coastal and offshore waters, based on the mechanism by which particles settle down at bathymetries below 20 m, and are transported back to the coast (see Fig.A5). By this mechanism, particles tend to accumulate in the coastal zone, which explains the continuous cross-shore gradient in SPM concentration.

5.4. Feedback effect of SPM dynamics on phytoplankton photosynthesis

Ou model study (see section 1.6) tends to confirm the importance of the EPS and TEP production by phytoplankton in the turbid Belgian coastal zone. As phytoplankton produces EPS, the flocculation of particles is enhanced in spring and summer, thus resulting in a higher light penetration in the water column (Fig.A7). This is in turn favorable to phytoplankton production. By comparing scenarios where the stickiness property of TEP is activated or not, the model shows a substantial increase in photosynthesis when TEP enhances particle flocculation.

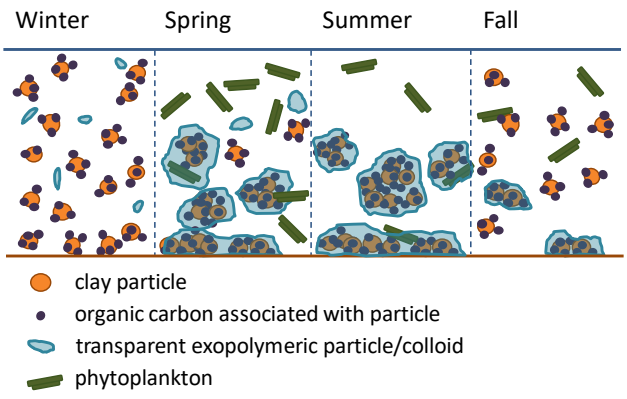

Figure A7 Seasonal variability in phytoplankton, TEP, and SPM concentrations in turbid waters. In spring and summer, the decrease in SPM concentration in the water column promotes better light penetration and increased photosynthesis by phytoplankton. In autumn, fresh TEP is consumed by respiration more rapidly than it is produced. This leads to reduced flocculation and increased water turbidity, which impairs photosynthesis.

5.5. Particle dynamics drive part of the carbon cycle on shelf seas

Particle dynamics in the marine system drive part of the carbon cycle as they control the fate of particulate organic carbon (Fig.A8). Budgets of SPM can be made at the scale of the North Sea by combining information from satellite products of SPM concentration and the semi-empirical model describing the organic content of SPM (Fig.A9; and see Fig.A2a, and Schartau et al., 2019; Fettweis et al., 2022; Desmit et al., 2024). To establish the quantity of POC in the North Sea, it is also necessary to collect information on the vertical profiles of SPM and POC concentrations, and information on the stratification regime of each satellite pixel (see section 1.7).

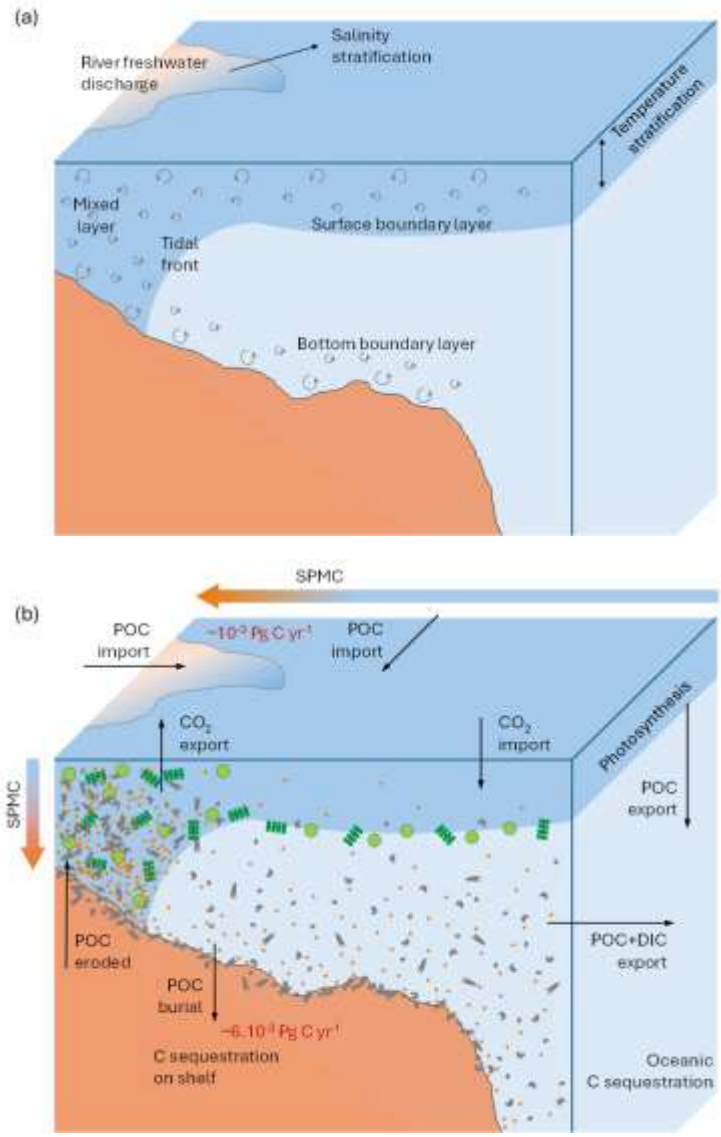

Figure A8 Representation of a shelf sea featuring a gradual increase in bathymetry from the coast toward the shelf break. (a) Description of hydrodynamics: surface waters are represented by dark blue and bottom waters by light blue; round arrows represent the propagation of turbulent energy in the water column. The water column shifts from well mixed to seasonally stratified as the bathymetry increases. (b) Description of particle dynamics (green: phytoplankton cells and colonies; grey: POC_{slow}; orange: clay particles; see Fig.A1).

Phytoplankton production occurs in well-mixed areas and around the pycnocline in stratified areas. Arrows represent the transport and exchange of organic and inorganic carbon within the system, or at the air-sea and sea-sediment interfaces (Thomas et al., 2004). Red numbers indicate established fluxes at the scale of the North Sea: POC import (adapted from Dobrynin, 2009 and Fettweis et al., 2007) and POC burial (adapted from Regnier et al., 2013). Hydrodynamics directly influence the SPM dynamics and the phytoplankton photosynthesis, both of which drive the fate of organic matter and, thus, influence the carbon cycle. Carbon sequestration (for at least 100 years) occurs when POC is buried in the sediment and when POC or DIC is exported toward the ocean interior.

While they are continuously subject to tidal settling and resuspension in well-mixed areas, particles obey different vertical distributions in the seasonally stratified areas of the shelf sea. In well-mixed waters, the vertical distribution of the SPM concentration can be seen as an exponential increasing toward the bottom and varying at tidal scale with current velocity. In thermally stratified waters, phytoplankton production takes place at the pycnocline (the lowest one in case of several levels of stratification), and the resulting POC settles in lower layers, while the shear stress on the sediment bed generates particle resuspension. The SPM concentration shows relatively low and vertically constant values in the surface mixed layer, increases progressively in the vicinity of the pycnocline, and shows relatively high and vertically constant values in deeper waters toward the bottom. The ratio between surface and bottom values can reach one order of magnitude in stratified areas like the Oysterground in the North Sea.

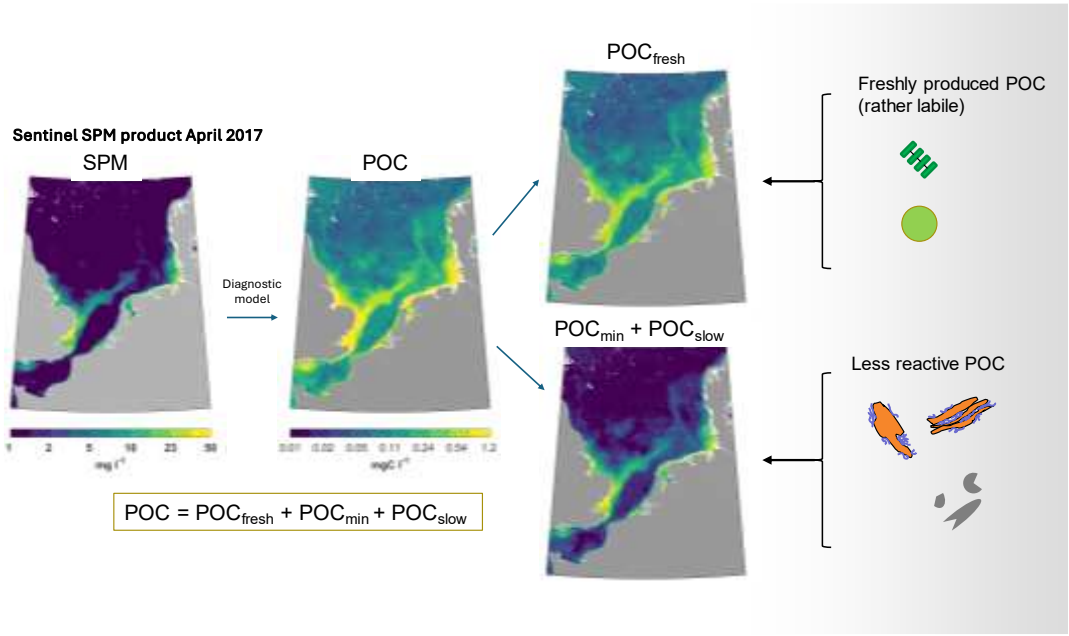

Figure A9 By combining satellite products and our semi-empirical model based on in situ data, the surface SPM concentration can be converted into surface POC and its components concentrations, here, POC_{fresh} and POC_{min}+POC_{slow}. Scales are not shown: at all seasons, POC_{min}+POC_{slow} largely dominate the POC_{fresh}, especially in winter.

The amount of organic carbon entering the North Sea from both the ocean and the adjacent rivers each year (~10^{-3} Pg C yr^{-1}) is of the same order of magnitude as the amount of buried organic carbon in shelf sediment (~6.10^{-3} Pg C yr^{-1}; see Fig.A8). The total mass of organic carbon present in suspension within the water column of the North Sea approaches these numbers (10^{-3} to 5.10^{-3} Pg C, respectively in summer and winter). A question not addressed in BG-PART is what is the fate of suspended organic carbon? Does it vary on the long term? Is it transported away, or does it deposit in the bottom sediment or in intertidal areas? These questions may be addressed in future research projects.